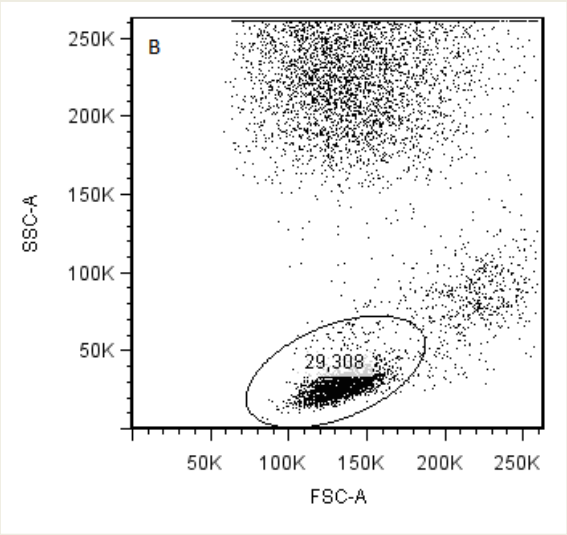

Figure 11. Gating strategy for lymphocyte gate used in blood concentration calculations. To ensure proper calculations of blood dendritic cell concentrations, a lymphocyte gate including B cells was used.

The blood monocyte enumeration was performed by a leukocyte gate (P1 region) and a monocyte gate (P2 region), both defined in the FSC/SSC plot, see Figure 12. The three subtypes of monocytes were found by changing the parameters of the P2 region to a FITC/PE plot, allowing division of the cells according to CD14 and CD16 expression. An acquisition threshold was set, and acquisition was performed until 10,000 evens or more were acquired in the P2 region.

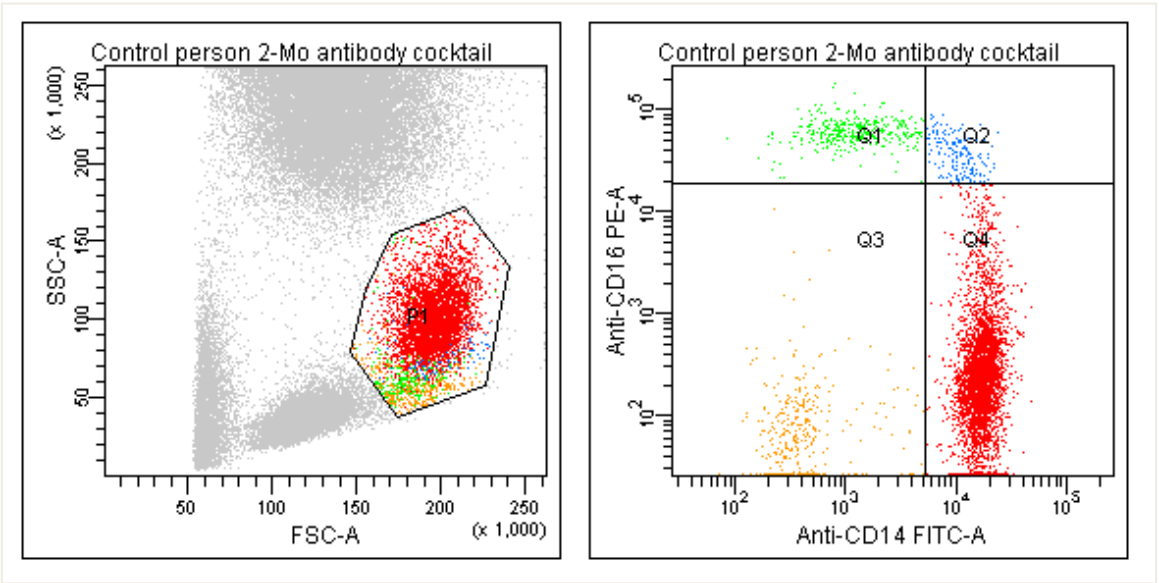

Figure 12. The gating strategy of blood monocyte subtype analysis. Left plot: Monocyte gate (P2) defined by FSC/SSC plot. Right plot: Nonclassical (Q1), intermediate (Q2) and classical monocytes (Q4) were found by their expression of CD14 and CD16 in a CD14 FITC/CD16 PE plot. Plots acquired from FACSDiva™ Software.

For investigation of monocytes in urine samples the first gate (P1) was set on CD45 positive cells in a FSC/CD45 plot (possible with the third approach of urine cell sample preparation). Subsequently, the

monocyte population was identified (P2) in a FSC/SSC plot of the P1 region. In cases of low numbers of cells in the P1 region monocytes could not be defined. Provided that the samples were prepared without the addition of CD45 (second approach) the P2 monocyte gate was made from the FSC/SSC plot directly, see Figure 13.

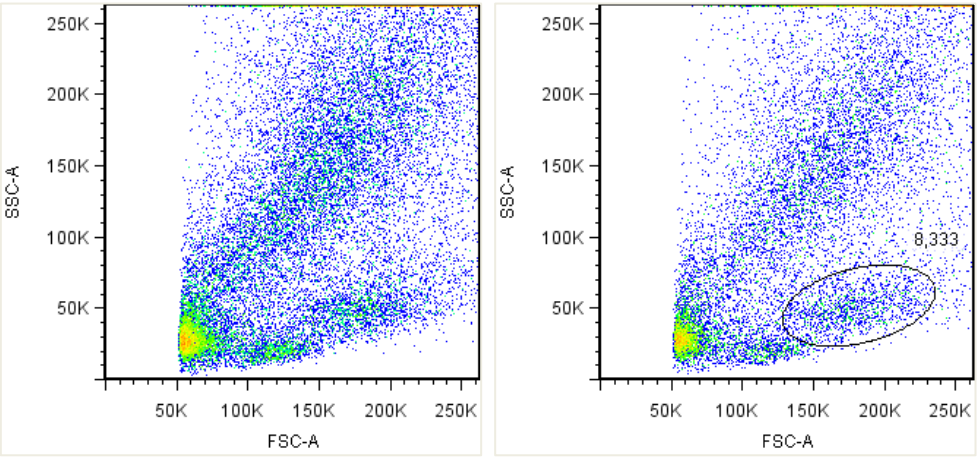

Figure 13. The gating strategy of urine monocyte analysis. Monocyte population (right picture) was located in a FSC/SSC plot (left picture) when samples was prepared by the second approach. Plots acquired from FlowJo™ software.

The populations from the flow cytometric analysis (dendritic cells and monocytes in whole blood and monocytes in urine) allowed analysis of their expression of HLA-DR and TLR4. Histogram overlays of APC-Cy-7and PE-Cy7, respectively, was made (see Figure 14 and Figure 15), and the difference between median fluorescence intensity for antibody and its isotype control was calculated.

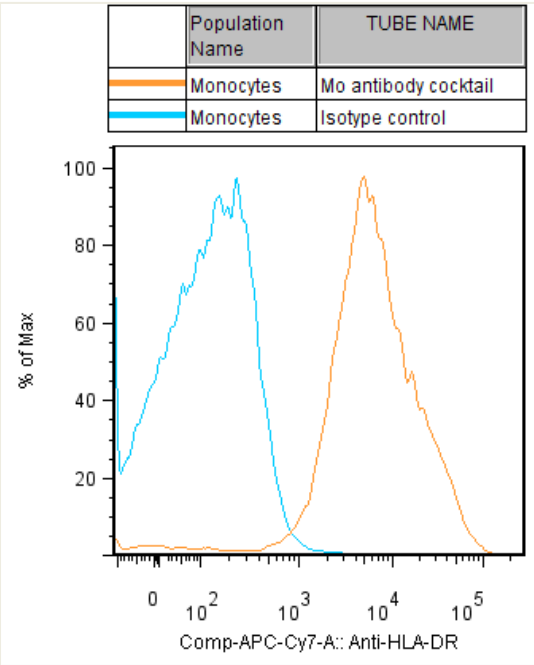

Figure 14. Histogram overlay of APC-Cy7 fluorescence intensity of monocytes stained with the monocyte antibody cocktail (orange curve) and monocytes stained with the isotype cocktail (blue curve). Y-axis: percent of total monocyte count in the sample. Data from control subject 1, day 21, FlowJo™ software.

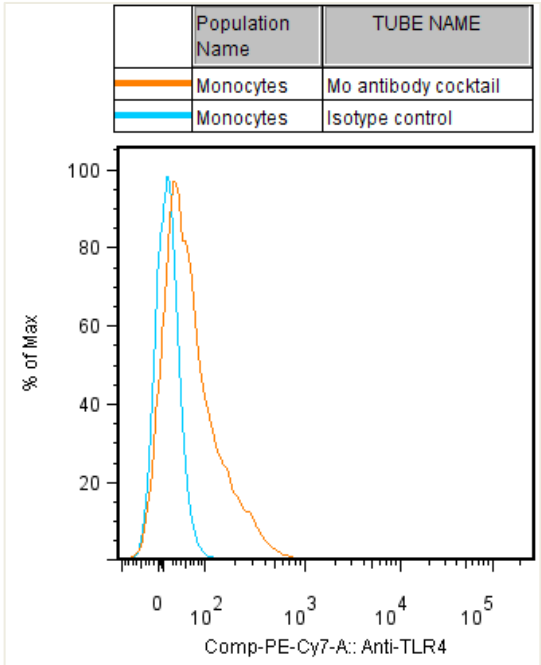

Figure 15. Histogram overlay of PE-Cy7 fluorescence intensity of monocytes stained with the monocyte antibody cocktail (orange curve) and monocytes stained with the isotype cocktail (blue curve). Y-axis: percent of total monocyte count in the sample. Data from control subject 1, day 21, FlowJo™ software.

Absolute Leucocyte Differential Counts

White blood cell differential counts were performed at The Department of Urology, Aalborg Hospital.

Results

Absolute Leucocyte Counts by Flow Cytometry and Absolute Leucocyte Differential Counts

One of the main objectives of the present study was to quantitate subpopulations of dendritic cells and monocytes in the blood of IgAN patients and control subjects. In addition to the relative quantity of these cell types, provided by standard flow cytometry, it was also an aim to determine the exact number of each cell type per ml of blood. For this purpose, a defined volume of blood was added to a tube containing a known number of BD TruCount™ beads prior to analysis. However, the use of BD TruCount™ beads to obtain absolute leucocyte counts was not successful. The problem was that normal, well defined populations of leucocytes could not be identified in FSC/SSC dotplots when using the BD TruCount™ tubes. Assuming this could be due to a problem with the lysing of erythrocytes, two different lysing solutions were tried, but this did not solve the problem, see Figure 16.

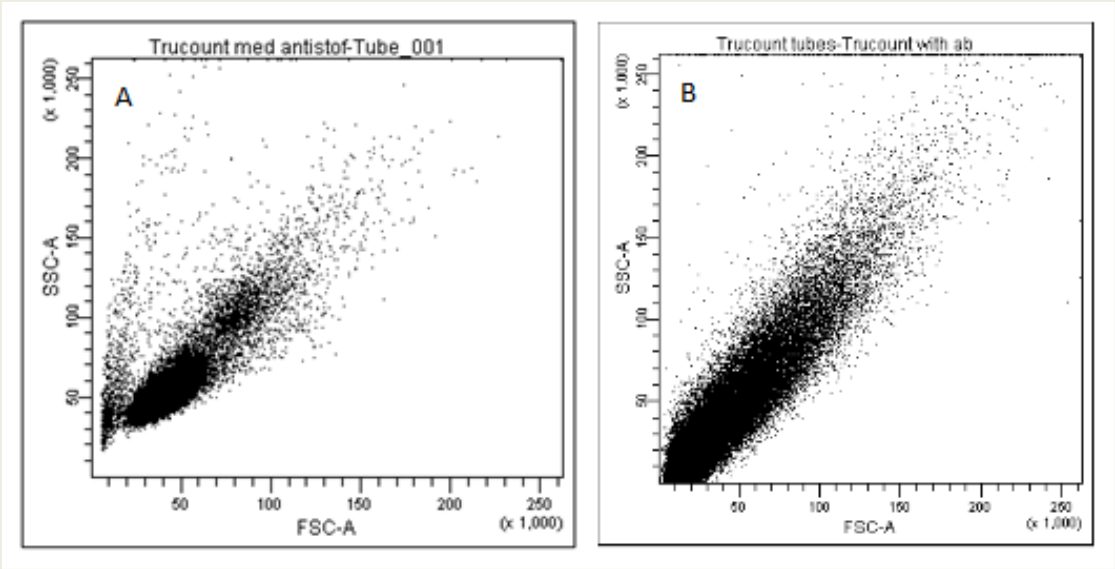

Figure 16. FSC/SSC plots of BD TruCount™ tubes. A. Red blood cells lysed with ACK lysing buffer. B. Red blood cells lysed with BD FACS Lysing Solution recommended by the manufacturer of the TruCount™ tubes. Graphs are generated from FlowJo™ software.

As an alternative, absolute differential cell counts of patient samples were provided by the Department of Urology, Aalborg Hospital (see Table 5), and percent wise distribution within parent gate, the concentration of monocyte and dendritic cell subpopulations in whole blood was calculated (see Table 6).

Patient 1				Patient 2			
Visit no.	Leucocyte count (x10^9/L)	Lymphocyte count (x10^9/L)	Monocyte count (x10^9/L)	Visit no.	Leucocyte count (x10^9/L)	Lymphocyte count (x10^9/L)	Monocyte count (x10^9/L)
1	5.9	1,91	0,44	**1**	5.9	1,19	0,24
2	7.8	2,54	0,52	**2**	6.8	1,51	0,1
3	6.2	2,57	0,42	**3**	8.6	3,08	0,17
4	8.2	3,37	0,63	-	-	-	-

Table 5. Absolute leucocyte differential counts (leucocytes, lymphocytes and monocytes) provided for the each visit of the two patients.

Subject Visit no.	CD1c$^+$ DC (x10^7/L)	CD303$^+$ DC (x10^7/L)	CD141$^+$ DC (x10^7/L)	Non-classical mo. (x10^7/L)	Intermediate mo. (x10^7/L)	Classical mo. (x10^7/L)
Patient 1 Visit 1	3,262	0,302	0,013	2,455	4,302	35,786
Patient 1 Visit 2	3,985	0,109	0,023	2,170	6,621	41,645
Patient 1 Visit 3	5,996	0,149	0,008	2,194	1,434	37,249
Patient 1 Visit 4	6,558	0,192	0,007	4,436	1,928	51,271
Patient 2 Visit 1	3,739	0,048	0,007	0,157	2,303	20,370
Patient 2 Visit 2	3,532	0,068	0,003	0,159	0,547	8,948

Table 6. The calculated concentrations of dendritic cell and monocyte subtypes in whole blood from patient 1 and patient2. Concentrations are calculated from the values of the absolute leucocyte differentiation count and the values of distribution within the parent gate (lymphocyte gate with B-cells included and monocyte gate, respectively).

The absolute leucocyte differential count showed the concentration of leucocytes, lymphocytes, and monocytes in blood of the patients. Graph 1 illustrates the blood concentration of leucocytes. Patient 1 had an increase in leucocyte blood concentration at the time of the second measurement, then the concentration decreased at third measurement. Both patients had an increase in leucocyte blood concentration towards the end of the period. The greatest difference between patients was seen at day 21.

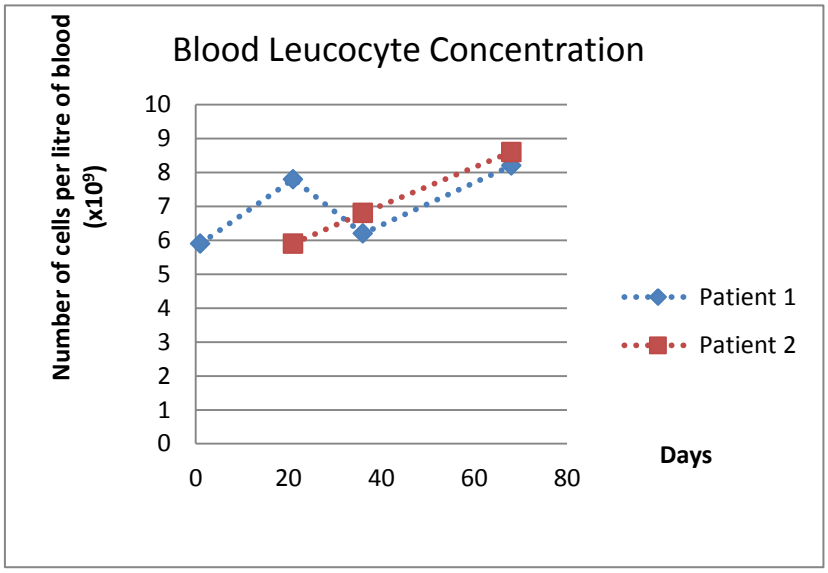

Graph 1. Blood leucocyte counts of the two patients (absolute leucocyte differential count). Data only available for the time points indicated by symbols. Dashed lines connect the symbols of each patient for the sake of clarity, only.

The blood lymphocyte concentration was higher in patient 1 compared to patient 2, see Graph 2.

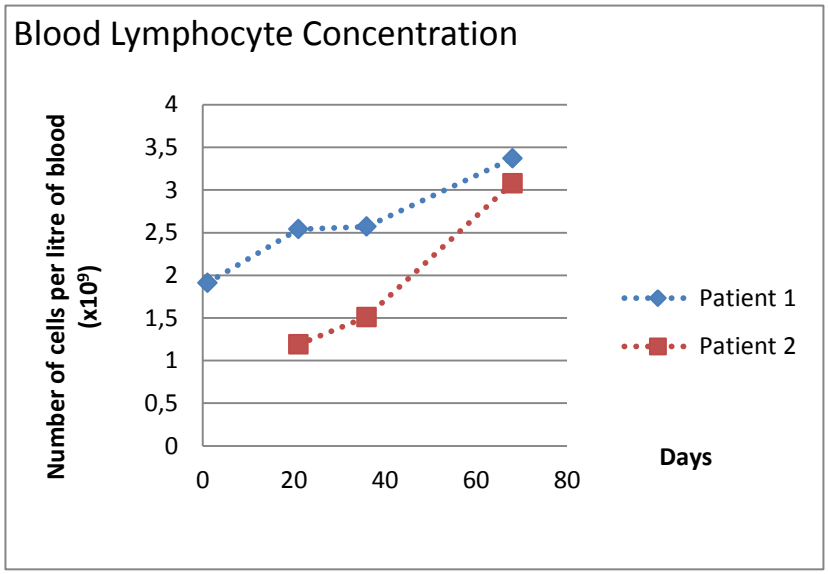

Graph 2. Blood lymphocyte counts of the two patients (absolute leucocyte differential count). Data only available for the time points indicated by symbols. Dashed lines connect the symbols of each patient for the sake of clarity, only.

The blood concentration of monocytes was low in patient 1, see Graph 3. The monocyte concentration of patient 1 decreased between the first and the last measurement. The lowest value was seen at the second measurement. Patient 2 showed an overall increase in the concentration of blood monocytes during the period. At the third day of testing the lowest value was seen.

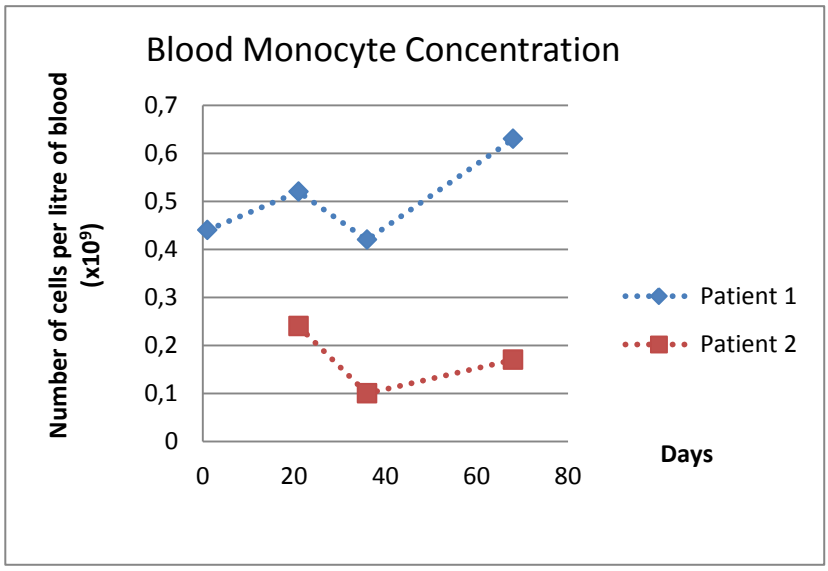

Graph 3. Blood monocyte counts of the two patients (absolute leucocyte differential count). Data only available for the time points indicated by symbols. Dashed lines connect the symbols of each patient for the sake of clarity, only.

Blood concentrations of non-classical, intermediate, and classical monocytes of patient 1 was all higher than those of patient 2 in all the days of testing (see Graph 4 to Graph 6). The non-classical monocyte blood concentration was increased in both patients at the time of the final test with the greatest increase seen for patient 1. Until day 36 the values were rather stable in both patients.

In patient 1 a decrease in intermediate monocyte concentration occurred at day 36 compared to the value of day 21. Patient 2 also had a lower value of day 36 compared to day 21. The difference between patients was greatest at day 21, and smallest at day 36, see graph 5.

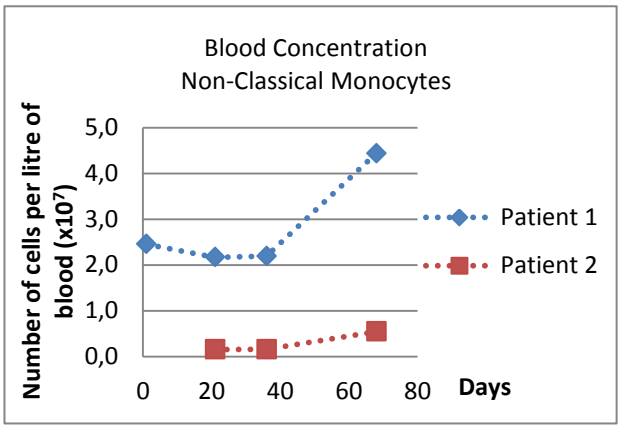

Graph 4. Blood concentration of non-classical monocytes of the two patients. Data only available for the time points indicated by symbols. Dashed lines connect the symbols of each patient for the sake of clarity, only.

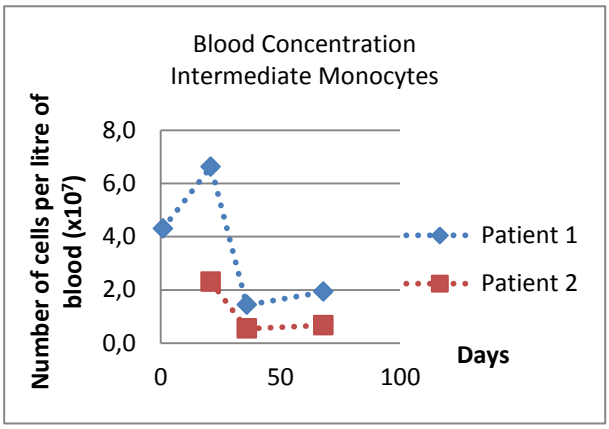

Graph 5. Blood concentration of intermediate monocytes of the two patients. Data only available for the time points indicated by symbols. Dashed lines connect the symbols of each patient for the sake of clarity, only.

As seen in Graph 6, the concentration of classical monocytes of patient was elevated compared to patient 2. The development of concentrations of patient 2 was similar to that of the intermediate monocytes.

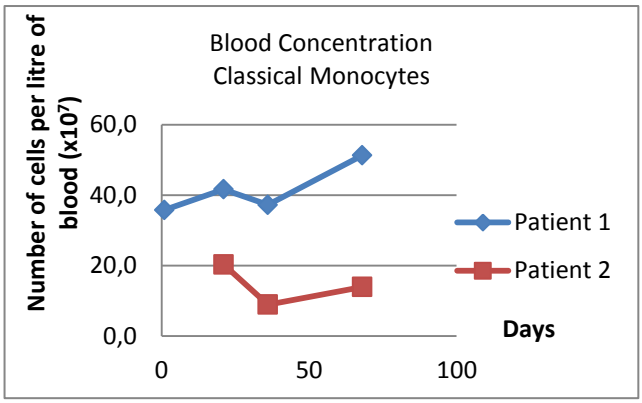

Graph 6. Blood concentration of classical monocytes of the two patients. Data only available for the time points indicated by symbols. Dashed lines connect the symbols of each patient for the sake of clarity, only.

Dendritic cell subset concentrations of blood are illustrated in Graph 7 to Graph 9. As seen with the monocyte subpopulations, the values of $CD303^+$ and $CD141^+$ subpopulationss in patient 1 were higher than those of patient 2. The number of $CD303^+$ dendritic cells was at day 1 of patient 1 compared to the values of the rest of the tests and of patient 2, see Graph 7.

Regarding the concentration of $CD1c^+$ dendritic cells the values of the two patients did not differ much, except for an elevated value of patient 2, day 68, in comparison with the rest of the concentrations of both patients, see Graph 8.

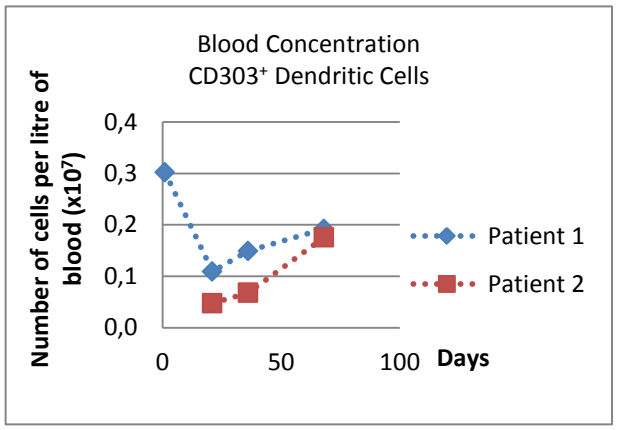

Graph 7. Blood concentration of $CD303^+$ dendritic cells of the two patients. Data only available for the time points indicated by symbols. Dashed lines connect the symbols of each patient for the sake of clarity, only.

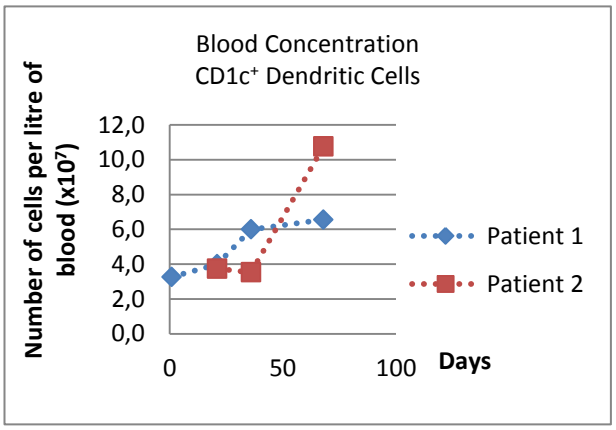

Graph 8. Blood concentration of $CD1c^+$ dendritic cells of the two patients. Data only available for the time points indicated by symbols. Dashed lines connect the symbols of each patient for the sake of clarity, only.

The concentration of $CD141^+$ dendritic cells differed only little within the measurements of patient 2. Patient 1, however, showed a concentration that differed in a larger scale between measurements, see Graph 9.

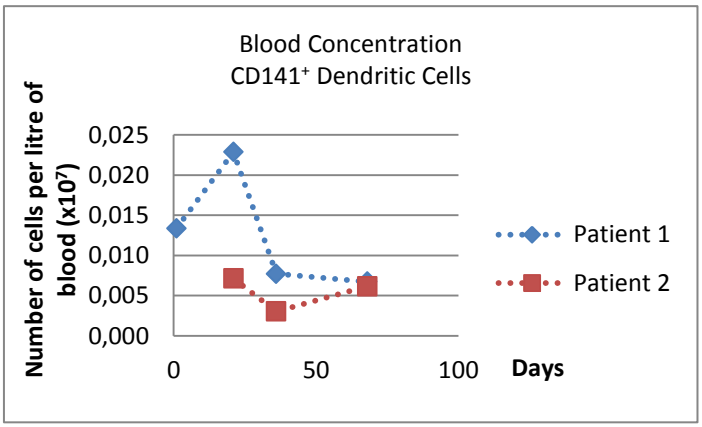

Graph 9. Blood concentration of $CD141^+$ dendritic cells of the two patients. Data only available for the time points indicated by symbols. Dashed lines connect the symbols of each patient for the sake of clarity, only.

Dendritic Cell Subset Enumeration in Whole Blood

The populations and gating of dendritic cells are illustrated in Figure 17 in which the data from one representative sample is shown. The corresponding plots obtained from the same sample with isotype controls are shown in Figure 18.

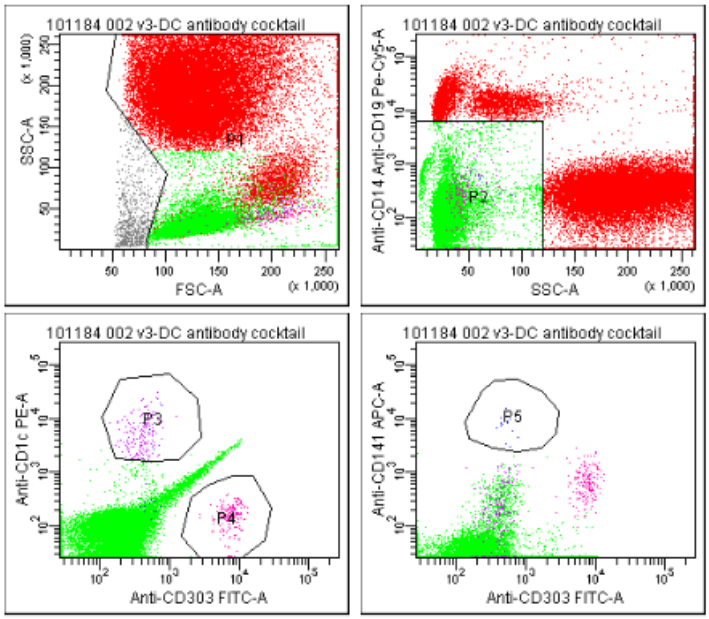

Figure 17. Populations and gates of the dendritic cell subset enumeration. P1: Leucocyte gate. P2: Lymphocyte gate. P3: CD1c$^+$ dendritic cell gate. P4: CD303$^+$ dendritic cell gate. P5: CD141$^+$ dendritic cell gate. Data from one representative sample is shown. Plots are generated from FACSDiva™ software.

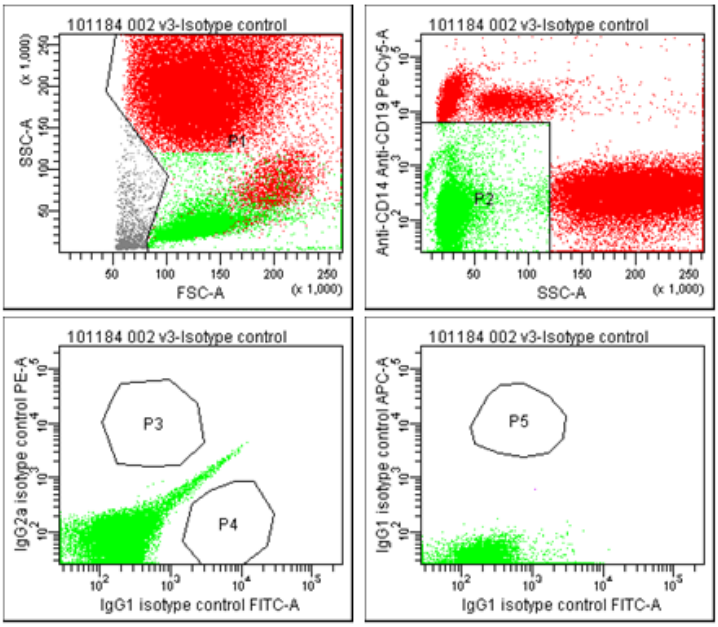

Figure 18. Populations and gates of the dendritic cell subset enumeration of the isotype control sample. P1: Leucocyte gate. P2: Lymphocyte gate. P3: CD1c$^+$ dendritic cell gate. P4: CD303$^+$ dendritic cell gate. P5: CD141$^+$ dendritic cell gate. Data from one representative sample is shown. Plots are generated from FACSDiva™ software.

Distribution of CD1c+, CD303+ and CD141+ Dendritic Cells

Dendritic cell subpopulation distribution can be seen in Graph 10 to Graph 13. The graphs illustrate mean distribution of dendritic cell subpopulations for each subject. In general, the distribution of dendritic cells was as follows; $CD141^+$ dendritic cells represented as the smallest subpopulation followed by $CD1c^+$ dendritic cells. The $CD303^+$ dendritic cells comprised the largest subpopulation. The exception was seen in patient 1 with a slightly higher percentage of $CD1c^+$ dendritic cells than $CD303^+$ dendritic cells.

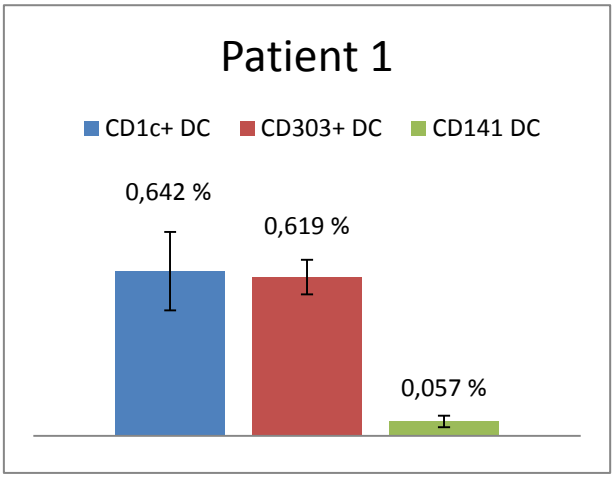

Graph 10. Mean distribution of dendritic cell subtypes in patient 1. The numbers indicate mean percent of leucocyte gate. Standard deviation between the days of testing is shown. DC: dendritic cell.

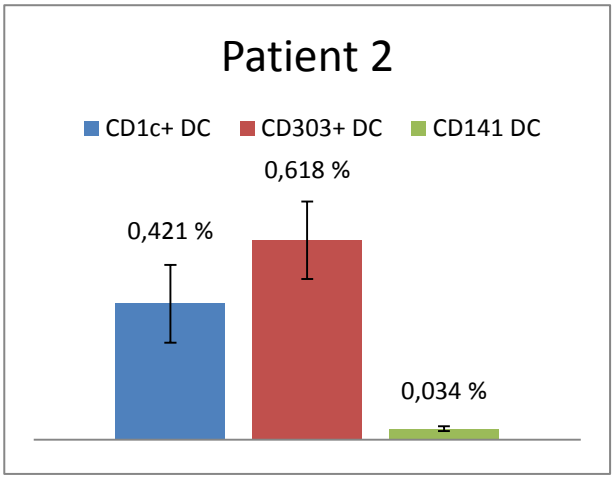

Graph 11. Mean distribution of dendritic cell subtypes in patient 2. The numbers indicate mean percent of leucocyte gate. Standard deviation between the days of testing is shown. DC: dendritic cell.

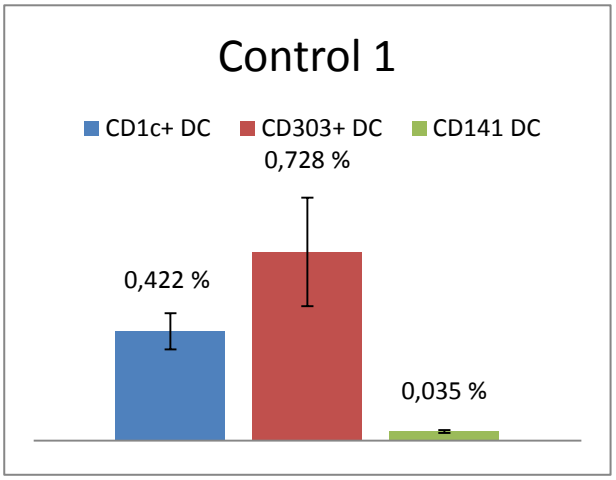

Graph 12. Mean distribution of dendritic cell subtypes in control subject 1. The numbers indicate mean percent of leucocyte gate. Standard deviation between the days of testing is shown. DC: dendritic cell.

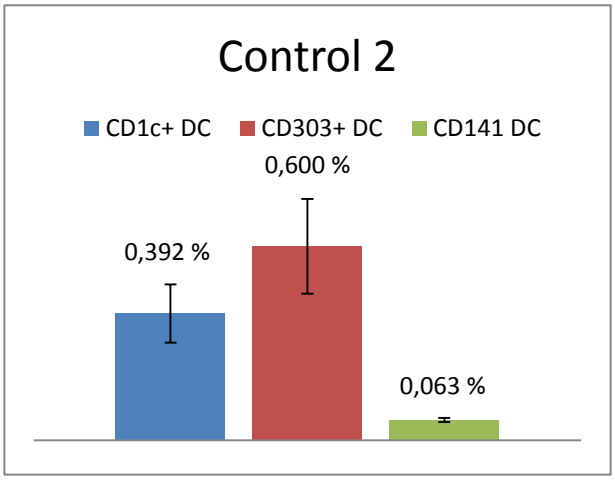

Graph 13. Mean distribution of dendritic cell subtypes in control subject 2. The numbers indicate mean percent of leucocyte gate. Standard deviation between the days of testing is shown. DC: dendritic cell.

Dendritic Cell Subclass Distribution over Time

The development in distribution of the dendritic cell subpopulations in the experimental period is shown in Graph 14 to Graph 19. Between patients there was a difference of approximately 0.4 percentage points in the size of $CD1c^+$ subpopulation up to day 36, see Graph 14. At the last day of testing, the subpopulation was rather similar in the two patients. Samples from the two control subjects differed less by a maximum of approximately 0.2 percentage points regarding the CD1c subpopulation, see graph 15. Patient 1 seemed to reach the highest value compared to patient 2, and control subject 1 and 2 during the period of testing.

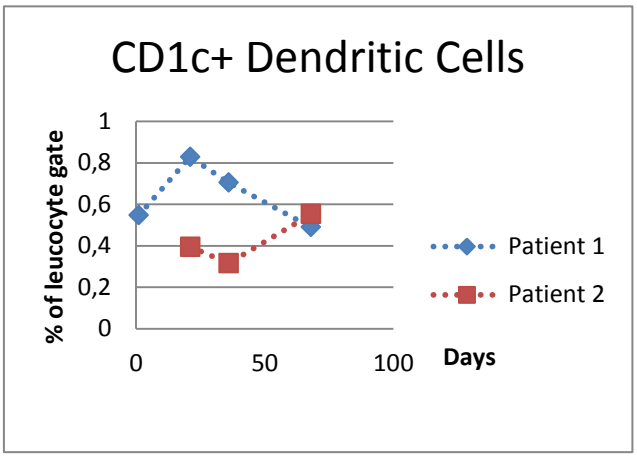

Graph 14. Distribution of $CD1c^+$ dendritic cells in patients. Data only available for the time points indicated by symbols. Dashed lines connect the symbols of each patient for the sake of clarity, only.

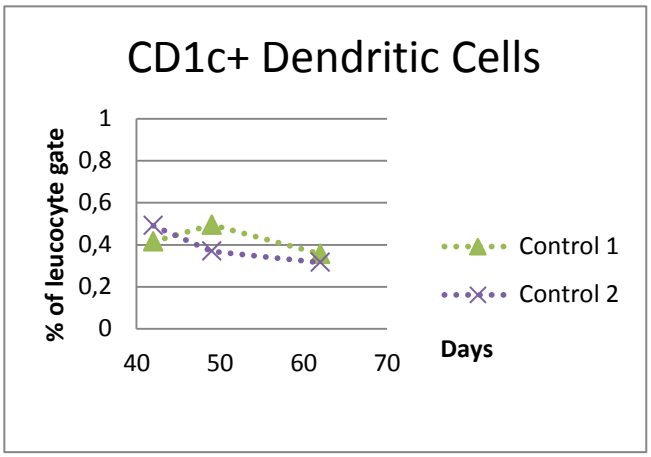

Graph 15. Distribution of $CD1c^+$ dendritic cells in control subjects. Data only available for the time points indicated by symbols. Dashed lines connect the symbols of each control subject for the sake of clarity, only.

The $CD303^+$ subtype was, as mentioned, the largest of the dendritic cell subtypes. Between all subjects the values differed by approximately 0.4 percentage points (see Graph 16 and Graph 17), and the greatest change during the period of testing was seen in control subject 1.

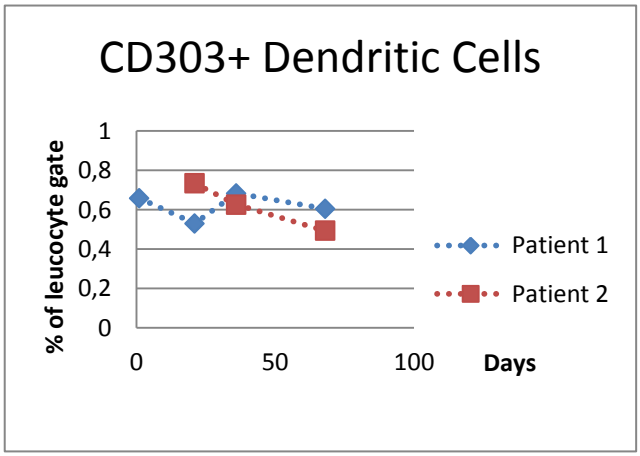

Graph 16. Distribution of $CD303^+$ dendritic cells in patients. Data only available for the time points indicated by symbols. Dashed lines connect the symbols of each patient for the sake of clarity, only.

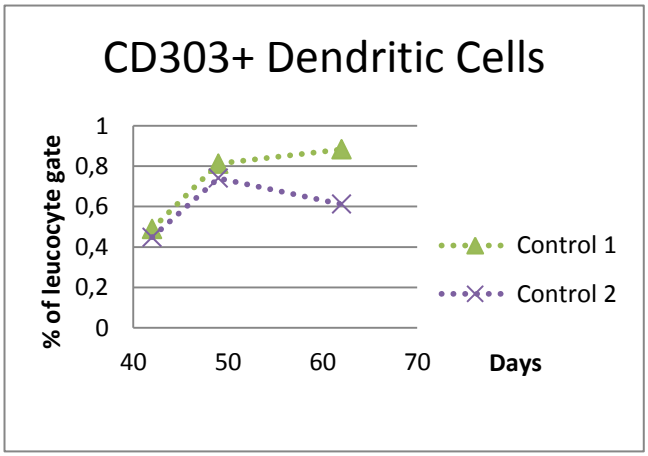

Graph 17. Distribution of $CD303^+$ dendritic cells in control subjects. Data only available for the time points indicated by symbols. Dashed lines connect the symbols of each control subject for the sake of clarity, only.

The difference in the CD141$^+$ dendritic cells between subjects reached a maximum of approximately 0.55 percentage points; see Graph 18 and Graph 19. Patient 1 reached the highest percentage of CD141$^+$ dendritic cells at the second testing, and as with the CD1c$^+$ dendritic cells the value decreased from that point with approximately 0.5 percentage points towards the end of the period. The difference between days of testing of patient 2 and control subjects 1 and 2 was less distinct compared to patient 1.

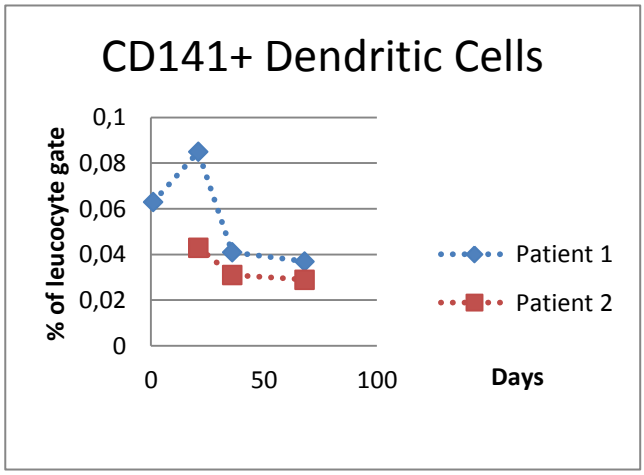

Graph 18. Distribution of CD141$^+$ dendritic cells in patients. Data only available for the time points indicated by symbols. Dashed lines connect the symbols of each patient for the sake of clarity, only.

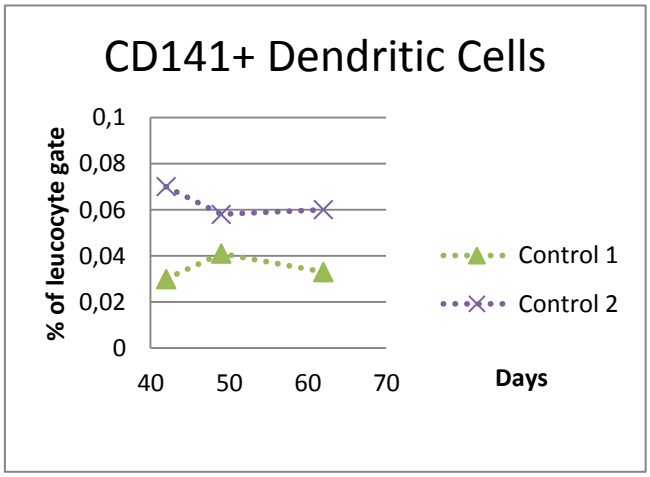

Graph 19. Distribution of CD141$^+$ dendritic cells in control subjects. Data only available for the time points indicated by symbols. Dashed lines connect the symbols of each control subject for the sake of clarity, only.

TLR4 Expression of Dendritic Cell Subpopulations

In order to monitor TLR4 expression, cells were stained with anti-TLR4 antibody. TLR4 expression of the dendritic cell subclasses is shown in Graph 20 to Graph 23. The highest TLR4 expression of patient 1 was seen at day one with CD1c$^+$ cells expressing most TLR4. This level of TLR expression by dendritic cells was the highest seen between subjects. At day 21 an overall decrease was seen for all three subtypes and a small increase of CD303$^+$ and CD141$^+$ expression occured at day 68. At day 36 and 68 the TLR4 expression of CD1c$^+$ dendritic cells was negative, indicating higher isotype fluorescence than that of the anti-TLR4 antibody sample.

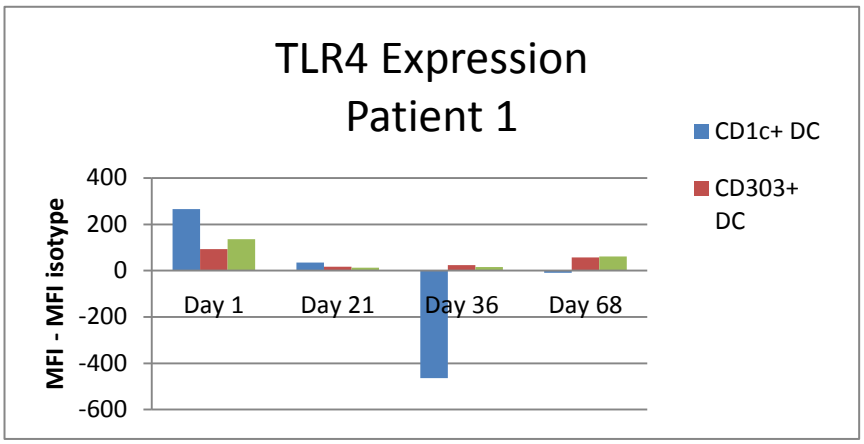

Graph 20. TLR4 expression of dendritic cell subtypes in patient 1.

Values of TLR4 expression in patient 2 also appeared to be negative for $CD1c^+$ and $CD141^+$ cells, respectively, at day 21 and 36 of the period. The highest value of TLR4 expression of $CD303^+$ dendritic cells was seen at day 68. At this time, low TLR4 expression of $CD1c^+$ dendritic cells occurred, see Graph 21.

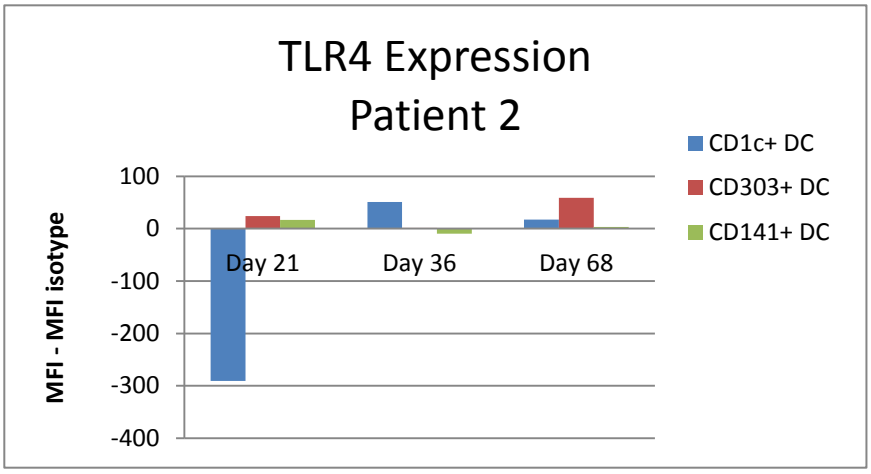

Graph 21. TLR4 expression of dendritic cell subtypes in patient 2.

Control subject 1 showed a decrease in TLR4 expression by $CD1c^+$ dendritic cells in time, and an increase in $CD303^+$ expression. The expression level of $CD141^+$ cells was stable in general. At day 62 the value of $CD1c^+$ cells was negative.

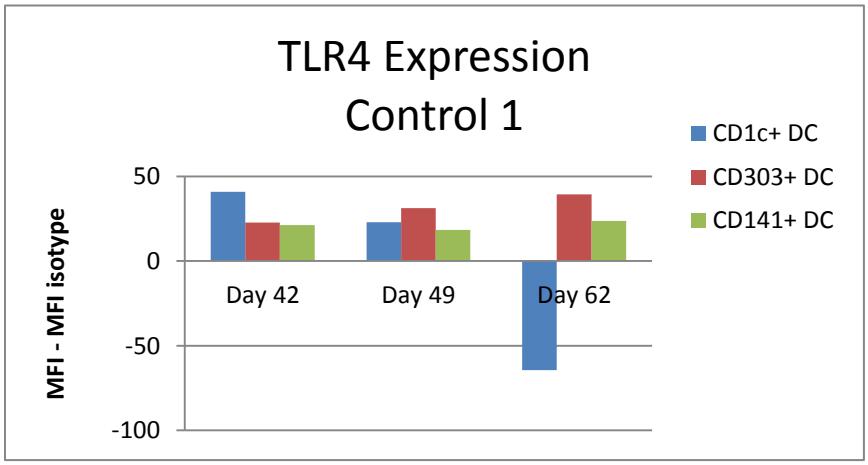

Graph 22. TLR4 expression of dendritic cell subtypes in control subject 1.

Several TLR4 expression values of control subject 2 subpopulations were negative, see Graph 23. These included that of $CD1c^+$ expression, day 42 and 49, and of $CD303^+$ day 42. In general, values were raised for the expression of all three subtypes at day 62.

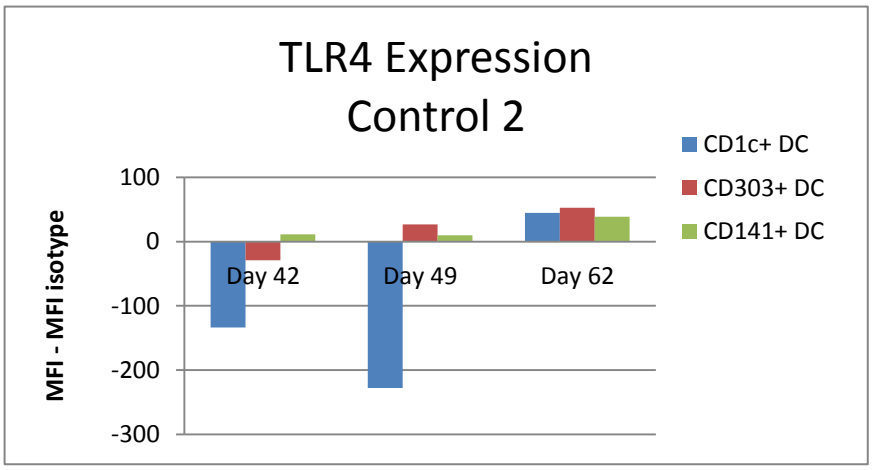

Graph 23. TLR4 expression of dendritic cell subtypes in control subject 2.

HLA-DR Expression of Dendritic Cell Subpopulations

HLA-DR expression of dendritic cell subtypes showed to be consistent between all samples. $CD1c^+$ dendritic cells expressed most HLA-DR, see Graph 24 to Graph 27. Except for patient 1, $CD303^+$ cells showed an expression level in between that of $CD1c^+$ cells and $CD141^+$ cells in general, with $CD141^+$ cells being the subpopulation having the lowest expression. $CD1c^+$ expression was high in the control subjects compared to the two patients.

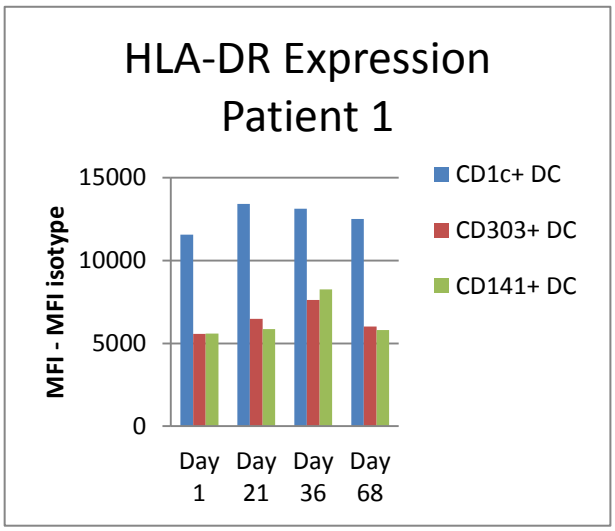

Graph 24. HLA-DR expression of dendritic cell subtypes in patient 1.

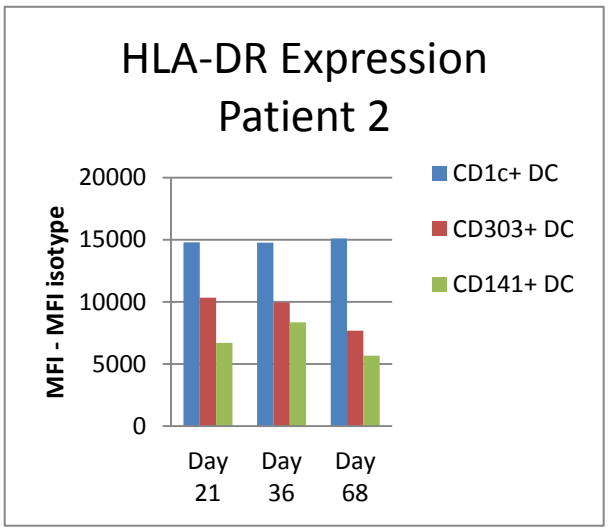

Graph 25. HLA-DR expression of dendritic cell subtypes in patient 2.

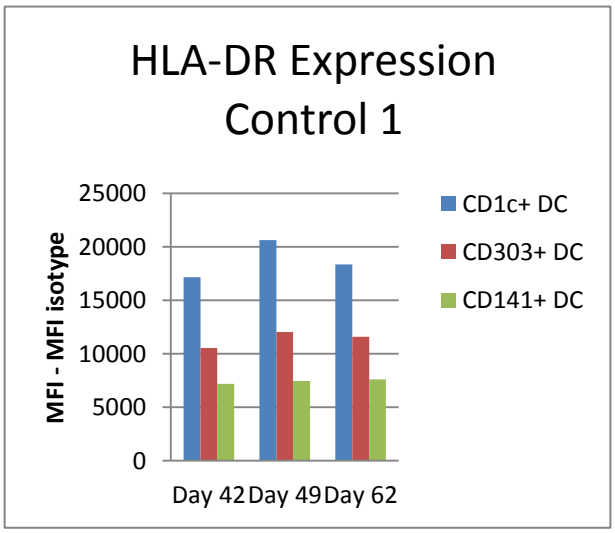

Graph 26. HLA-DR expression of dendritic cell subtypes in control subject 1.

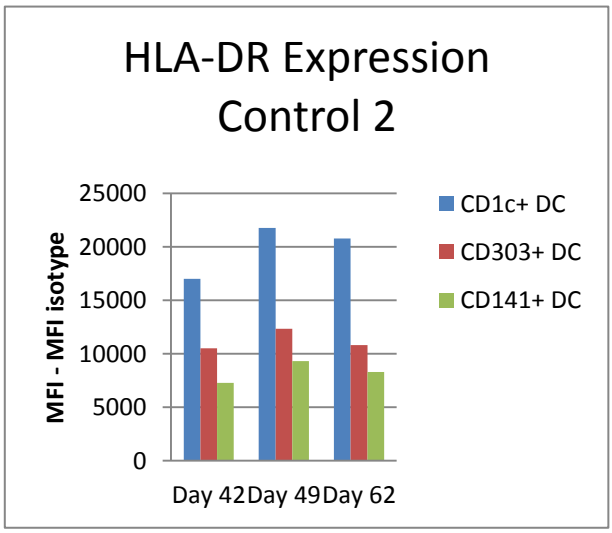

Graph 27. HLA-DR expression of dendritic cell subtypes in control subject 2.

Monocyte Subset Enumeration in Whole Blood

The populations and gating of non-classical, intermediate, and classical monocytes are illustrated in Figure 19 in which the data from one representative sample is shown. The corresponding plots obtained from the same sample stained with isotype controls are shown in Figure 20.

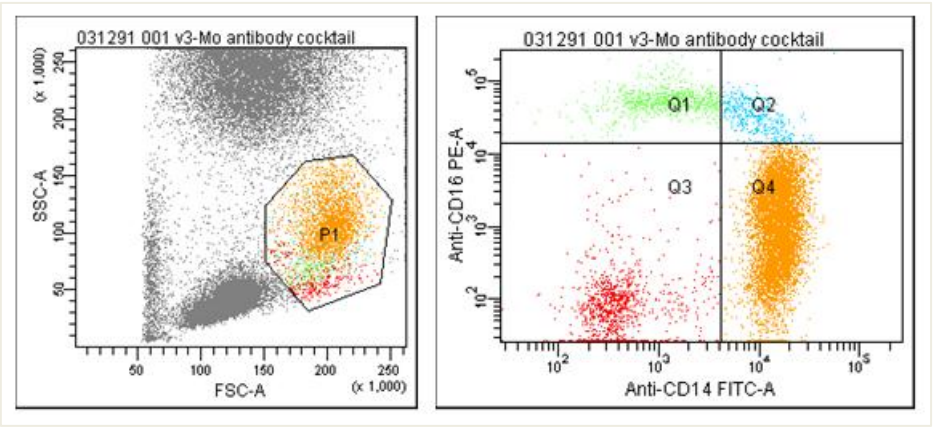

Figure 19. Populations and gates of the monocyte subset enumeration. P1: Monocyte gate. Q1: Non-classical monocytes. Q2: Intermediate monocytes. Q4: Classical monocytes. Data from one representative sample is shown. Plots are generated from FACSDiva™ software.

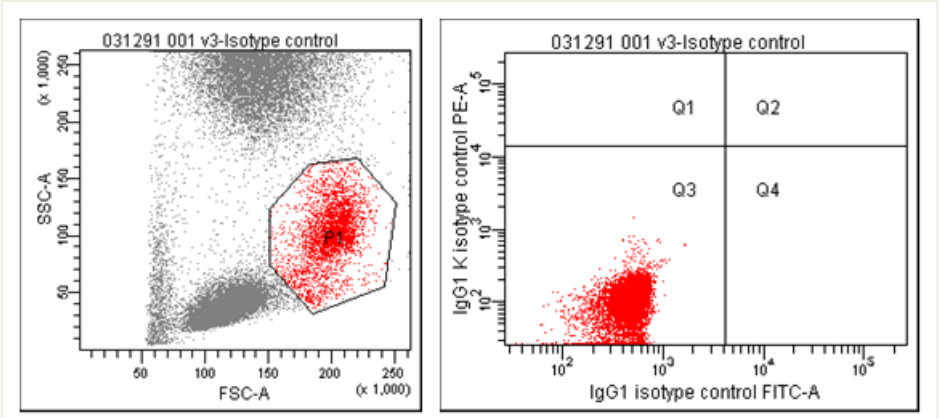

Figure 20. Populations and gates of the monocyte subset enumeration of the isotype control sample. P1: Monocyte gate. Q1: Non-classical monocytes. Q2: Intermediate monocytes. Q4: Classical monocytes. Data from one representative sample is shown. Plots are generated from FACSDiva™ software.

Distribution of Non-Classical, Intermediate, and Classical Monocytes

The distribution of non-classical, intermediate, and classical monocytes within the monocyte gate is shown in Graph 28 to Graph 31. The graphs illustrate mean distribution of monocyte subpopulations for each subject. Undetermined cells composed some of the cells of the monocyte gate, which explains why the percentages of the three subpopulations do not in total give a value of 100. The overall result was low numbers of non-classical and intermediate monocytes in comparison with the classical monocytes. Both patients had slightly higher average percentage of classical monocytes than control subjects. Patient 2 had a smaller frequency of non-classical monocytes than the other subjects.

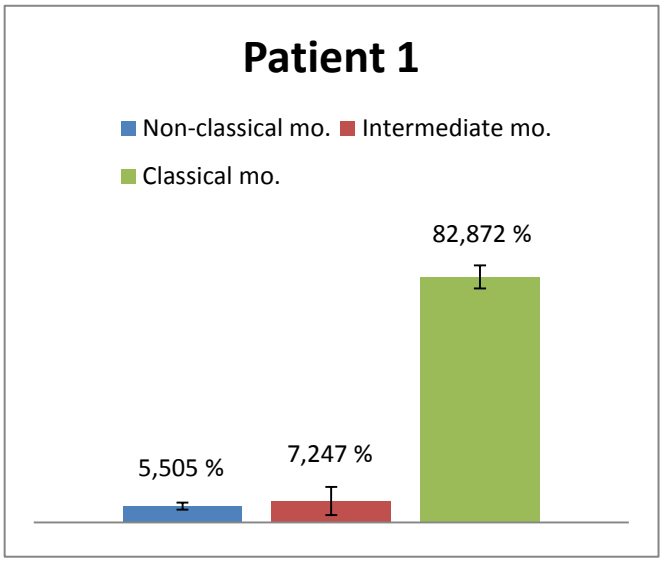

Graph 28. Mean distribution of monocyte subtypes in patient 1. The numbers indicate mean percentage of monocyte gate. Standard deviation between the days of testing is shown. Mo: monocyte.

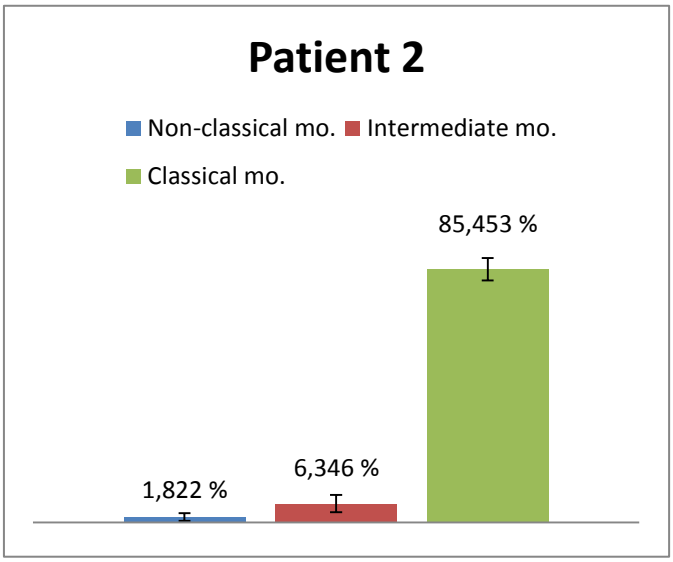

Graph 29. Mean distribution of monocyte subtypes in patient 2. The numbers indicate mean percentage of monocyte gate. Standard deviation between the days of testing is shown. Mo: monocyte.

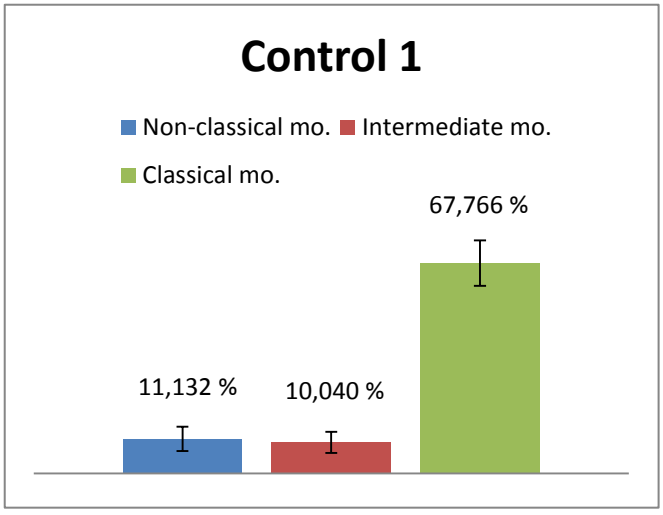

Graph 30. Mean distribution of monocyte subtypes in patient 1. The numbers indicate mean percentage of monocyte gate. Standard deviation between the days of testing is shown. Mo: monocyte.

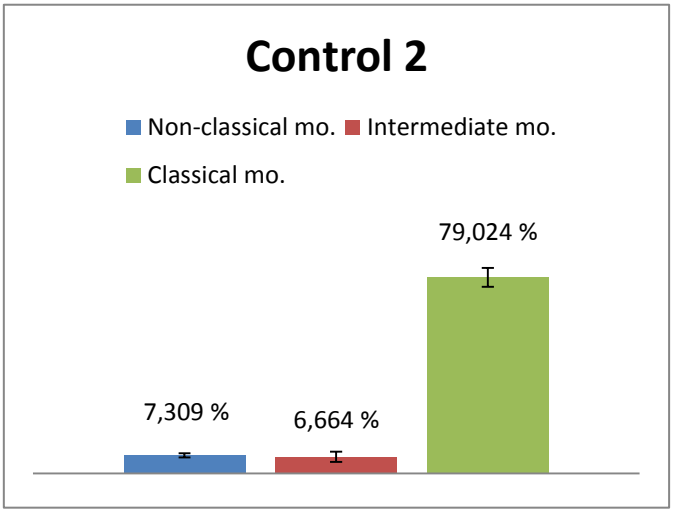

Graph 31. Mean distribution of monocyte subtypes in patient 1. The numbers indicate mean percentage of monocyte gate. Standard deviation between the days of testing is shown. Mo: monocyte.

Monocyte Subset Distribution over Time

The frequence of non-classical monocytes was in most instances higher in control subjects than in patients, see Graph 32 and Graph 33. Control subject 1 showed the greatest difference of approximately 3.5 percentage points between measurements. The non-classical monocyte subpopulation differed approximately 2.9 and 2.5 percentage points between samples of patient 1 and patient 2, respectively. The values of control subject 2 differed the least.

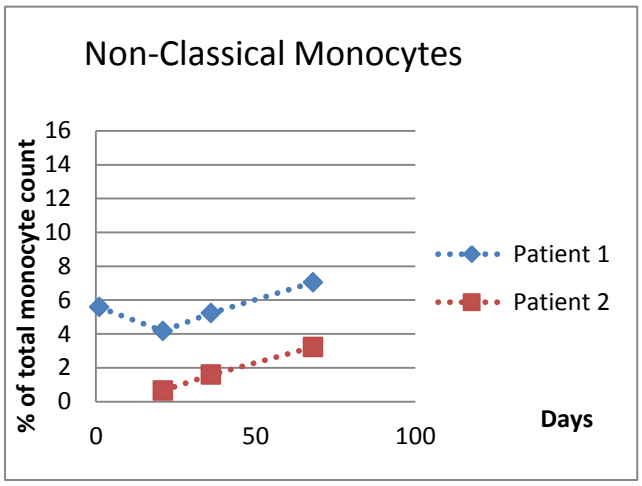

Graph 32. Distribution of non-classical monocytes in patients. Data only available for the time points indicated by symbols. Dashed lines connect the symbols of each patient for the sake of clarity, only.

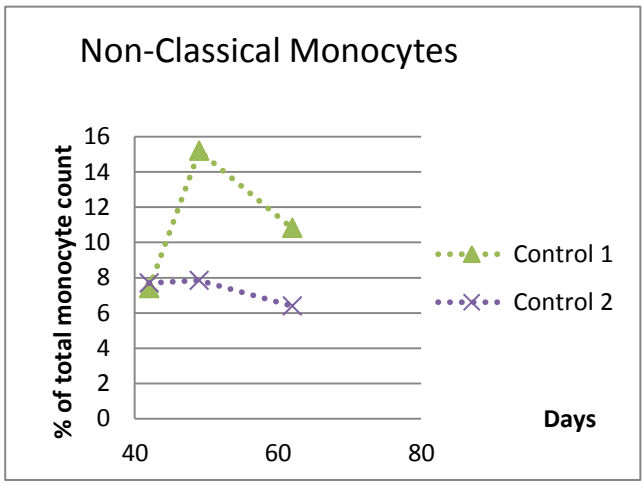

Graph 33. Distribution of non-classical monocytes in control subjects. Data only available for the time points indicated by symbols. Dashed lines connect the symbols of each control subject for the sake of clarity, only.

Regarding the classical monocytes, all samples showed a high frequency of this cell type. Control subjects had slightly lower values than did those of the patients, see Graph 34 and Graph 35.

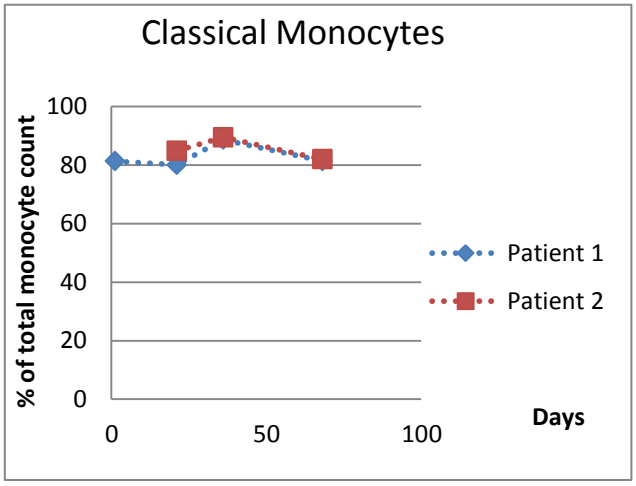

Graph 34. Distribution of classical monocytes in patients. Data only available for the time points indicated by symbols. Dashed lines connect the symbols of each patient for the sake of clarity, only.

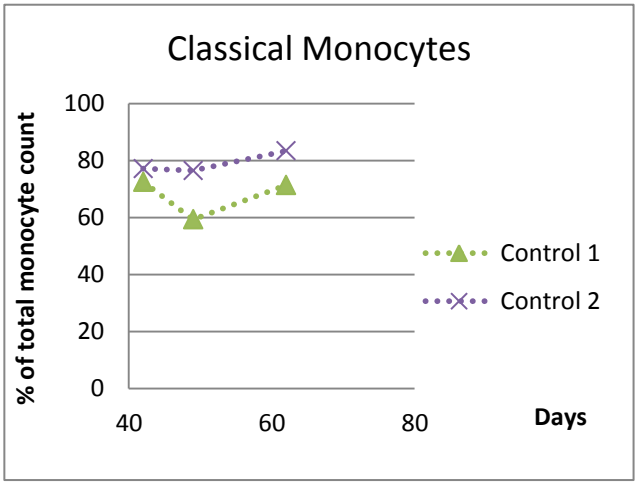

Graph 35. Distribution of classical monocytes in control subjects. Data only available for the time points indicated by symbols. Dashed lines connect the symbols of each control subject for the sake of clarity, only.

Great variations were seen in the distribution of intermediate monocytes – both between subjects and between samples of each subject. As with the $CD1c^+$ and $CD141^+$ dendritic cells, patient 1 had a decreasing frequency of intermediate monocytes when comparing early to late measurements. Patient 2 also showed a low number of intermediate monocytes in the last sample. Control subject 1 showed higher values than control subject 2 in two out of three measurements, see Graph 36 and Graph 37.

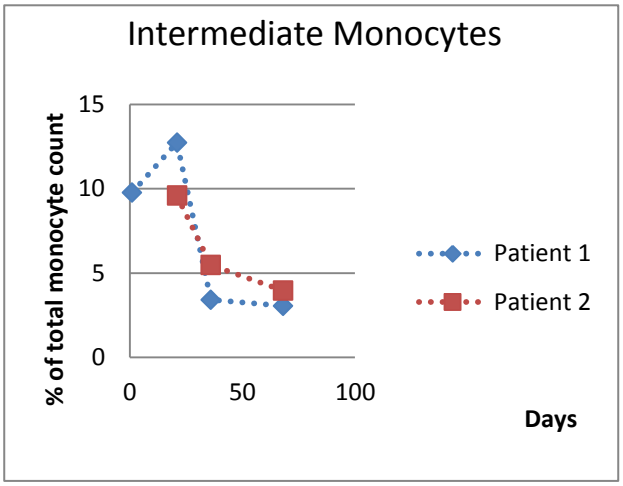

Graph 36. Distribution of intermediate monocytes in patients. Data only available for the time points indicated by symbols. Dashed lines connect the symbols of each patient for the sake of clarity, only.

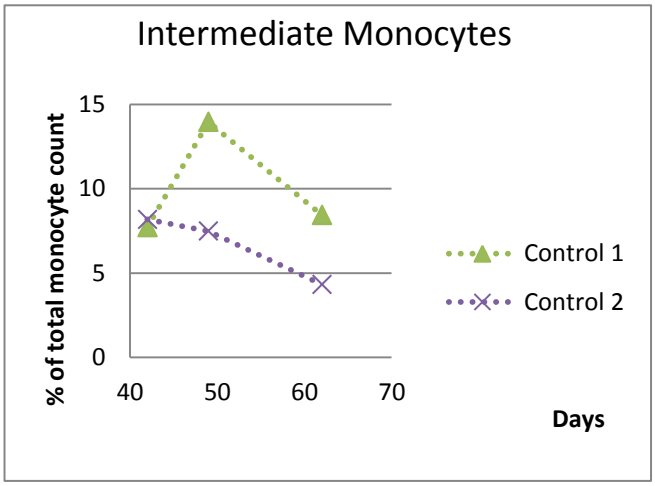

Graph 37. Distribution of intermediate monocytes in control subjects. Data only available for the time points indicated by symbols. Dashed lines connect the symbols of each control subject for the sake of clarity, only.

TLR4 Expression of Monocyte Subpopulations

The TLR4 expression of patient 1 did not show any negative values. The day 1 measurement showed higher values of TLR4 expression of all cell types compared with the following three measurements, see Graph 38. However, in the fluorescence intensity of patient 2 and both control subjects, negative values were revealed, see Graph 39 to graph 41. The intermediate monocytes of patient 1 showed highest TLR4 expression amongst monocyte subtypes at day 21, 36, and 68. This was also the case with patient 2, all measurements, and control subject 1, last two measurements. In control subject 2 there was higher TLR4 expression of the non-classical monocytes, than of the intermediate monocytes (Graph 41).

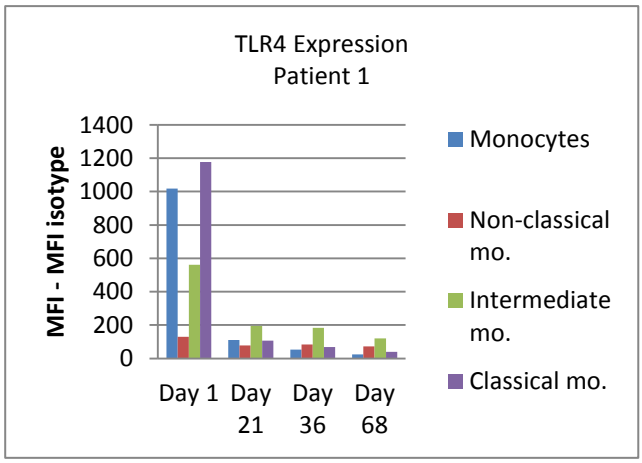

Graph 38. TLR4 expression of all monocyte subtypes in patient 1.

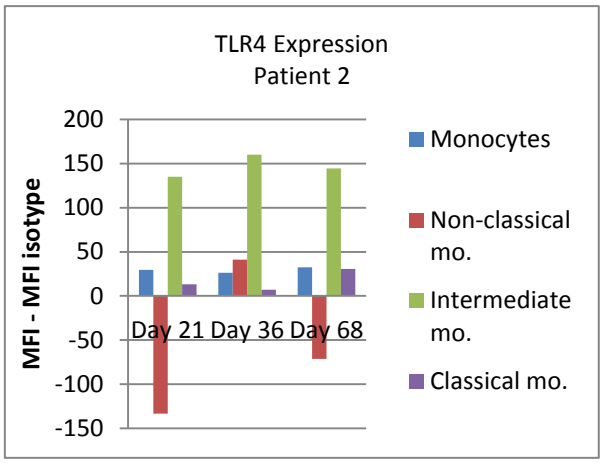

Graph 39. TLR4 expression of all monocyte subtypes in patient 2.

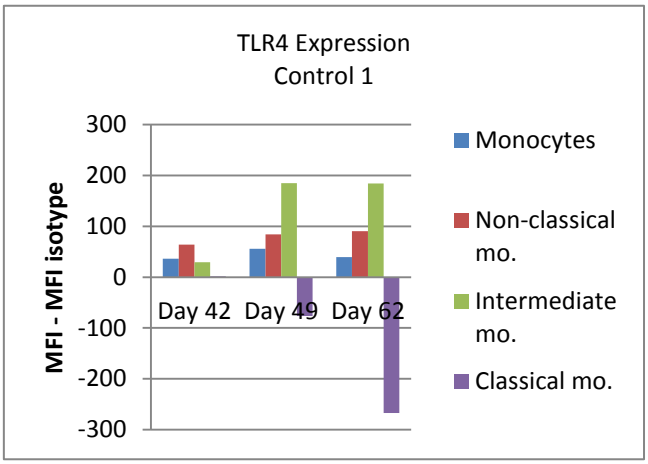

Graph 40. TLR4 expression of all monocyte subtypes in control subject 1.

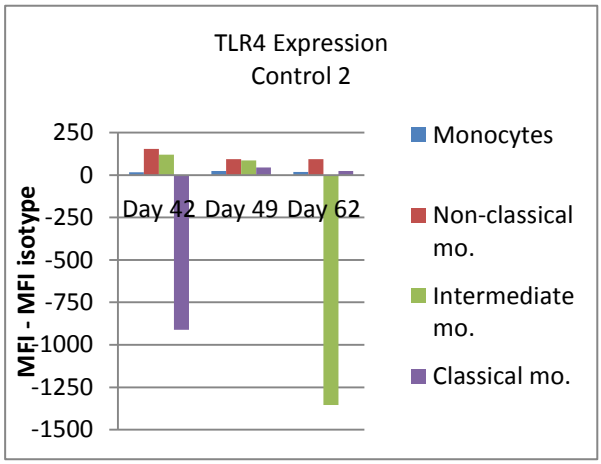

Graph 41. TLR4 expression of all monocyte subtypes in control subject 2.

HLA-DR Expression of Monocyte Subpopulations

Intermediate monocytes of all subjects expressed most HLA-DR, see Graph 42 to Graph 45. The maximum values of the intermediate monocytes differed between subjects, and the patients had lower maximum values than the control subjects. Compared to the other subtypes, HLA-DR expression was lowest for the classical monocytes, in general. One value, the one of day 42 of the classical monocytes was negative for control subject 2, see Graph 45.

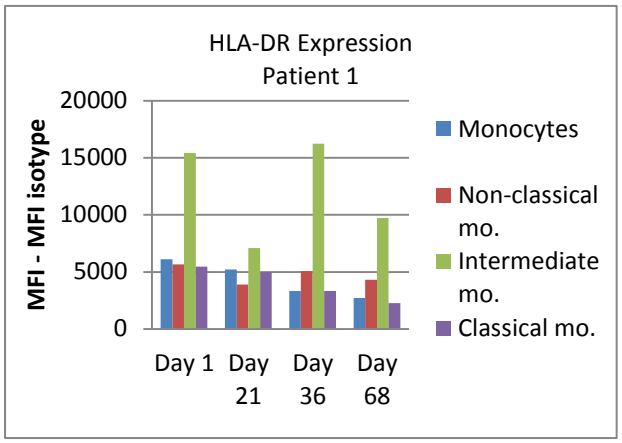

Graph 42. HLA-DR expression of all monocyte subtypes in patient 1.

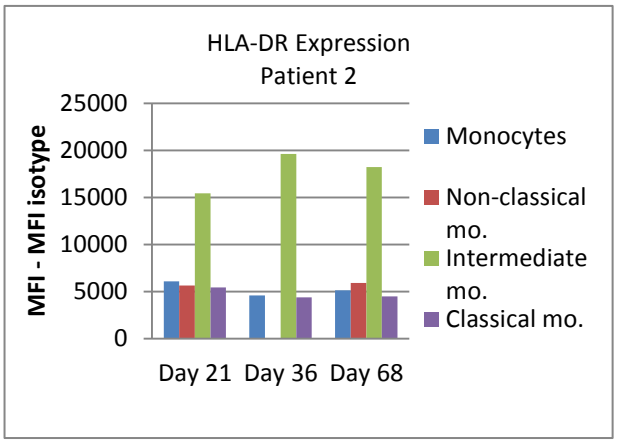

Graph 43. HLA-DR expression of all monocyte subtypes in patient 2

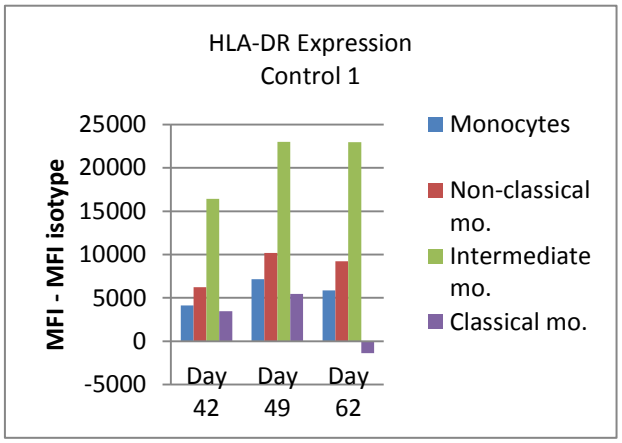

Graph 44. HLA-DR expression of all monocyte subtypes in control subject 1

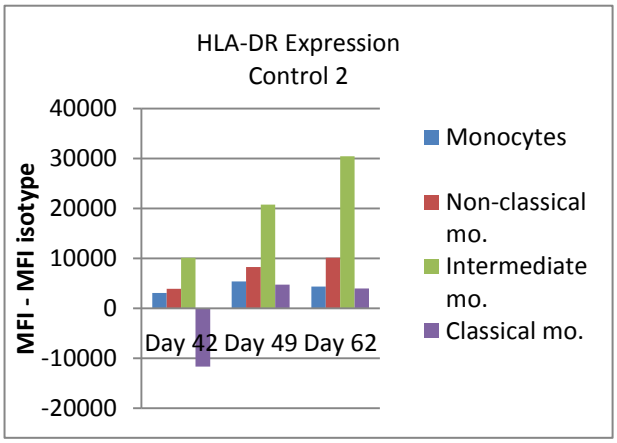

Graph 45. HLA-DR expression of all monocyte subtypes in control subject 2.

Monocyte Subset Enumeration in Urine

For flow cytometric analysis, the cells of urine samples were first concentrated by centrifugation and then the mononuclear cells in the concentrated sample were isolated by density gradient centrifugation. However, in samples from control subjects, no typical cell populations could be identified in FSC/SSC dotplots, see Figure 21.

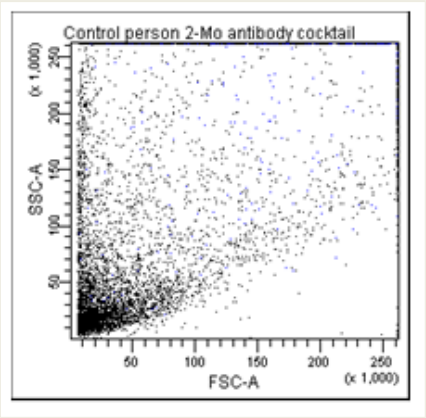

Figure 21. FSC/SSC plot for urine monocyte enumeration. The plot represents all samples of control subjects. 100% events are shown. Plot generated from FACSDiva™ software.

Urine monocytes were not found in patients when samples were not prepared with Lymphoprep™ and gradient centrifuged, which was the case of the first patient samples.

When changing the method of preparation, cell populations were seen. In the sample from patient 1, day 36, leucocyte subpopulations were located in a FSC/SSC plot, see Figure 22. When gating on the monocytes, the classical monocytes constituted the majority of monocytes. No sample was analyzed for patient 2 that day.

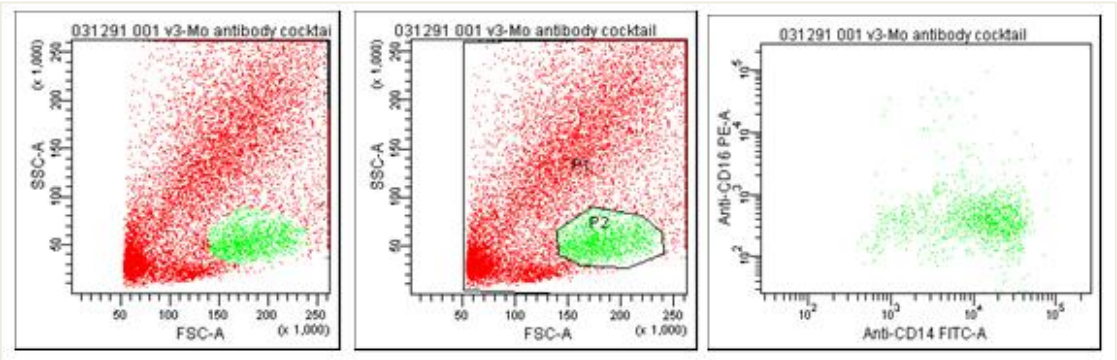

Figure 22. FSC/SSC plots for urine cells of patient 1, day 36, revealed the presence of leucocytes (left and middle plot). Classical monocytes seemed to be present in a CD14/CD16 plot (right plot). Sample preparation was according to approach no. 2. 100% of events are shown. Plots generated from FACSDiva™ software.

Classical monocytes was also observed in the urine of patient 1, day 68, see Figure 23. No monocyte population could be defined for patient 2, day 68. See Figure 24.

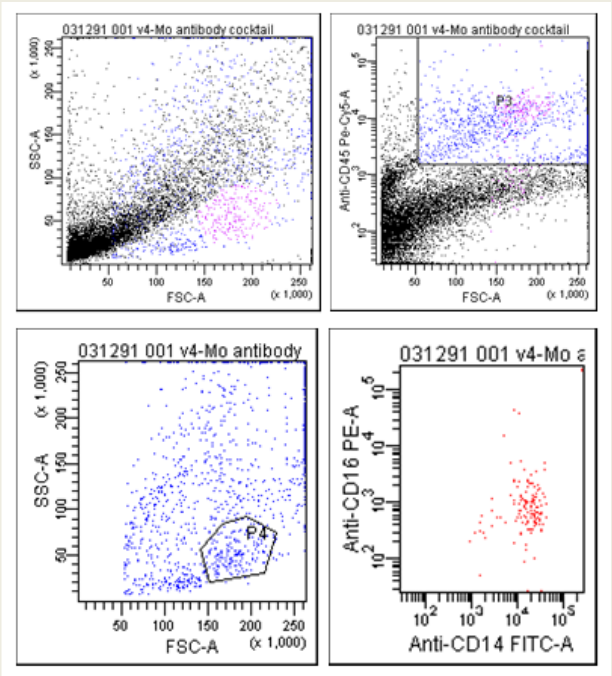

Figure 23. Upper left plot: FSC/SSC plot of urine cells of patient 1, day 68. Sample preparation was according to approach no. 3. Upper right plot: CD45-positive cells were localized. Lower left plot: FSC/SSC plot of CD45-positive cells revealed leucocyte populations, and a gate was set around monocytes. Lower right plot: CD14/CD16 plot revealed prescence of mainly classical monocytes. 100% events are shown. Plots generated from FACSDiva™ software.

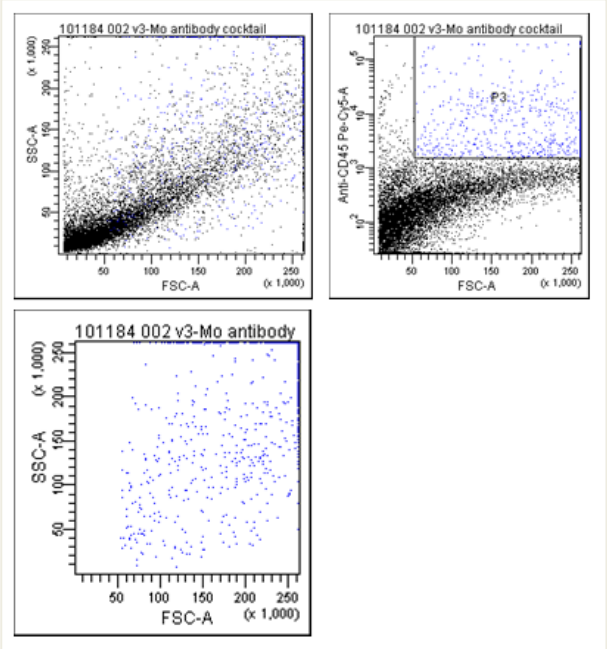

Figure 24. Upper left plot: FSC/SSC plot of urine cells of patient 2, day 68. Sample preparation was according to approach no. 3. Upper right plot: CD45-positive cells were localized. Lower left plot: FSC/SSC plot of CD45-positive cells revealed no leucocyte populations. 100% events are shown. Plots generated from FACSDiva™ software.

Discussion

The etiology of IgAN is still unknown, however immune mechanisms are crucially involved in the pathogenetic processes, and possibly the cause of the disease is also to be found within the immune system (5). The aim of the present project was to investigate monocyte and dendritic cell subpopulations in a group of IgAN patients and a group of controls.

Due to an unexpected delay in the approval process of the plans for the research project, a lower than expected number of suitable patients, and the fixed time allowed for a research project for the master's degree, only one third of the number of patients and controls anticipated, has been enrolled in the project. Obviously, this severely limits the conclusion that can be drawn on the basis of the results obtained.

Regarding enumeration of dendritic cell and monocyte subpopulations in IgAN patients and in healthy controls, the study has succeeded. In all subjects the subpopulations of cells were found. The monocyte and dendritic cell subpopulations being investigated in the present study have only recently been defined (3), and to our knowledge, the distribution of subpopulations within parent population of these cells in blood has not yet been investigated in IgAN. This makes the experimental setup of this study unique, and hence the results of it interesting.

The distribution of plasmacytoid CD303$^+$, myeloid CD141$^+$, and myeloid CD1c$^+$ dendritic cells, was consistent within control subjects. The CD303$^+$ dendritic cells constituted the largest group of the dendritic cell subpopulations, and CD141$^+$ cells accounted for the smallest fraction of subpopulations. In patient 1, the mean CD1c$^+$ subpopulation was increased in relation to the other subjects, see Graph 10 to Graph 13. However, based on the number of measurements it was not possible to establish a strong basis for describing tendencies of distribution in patients and in controls. In future studies the number of patients should therefore be increased and the period measurements prolonged.

This also applied to the distribution of monocytes. However a tendency of increased proportions of classical monocytes was seen in patients compared to control subjects. Mean percent wise distribution of the non-classical monocytes was decreased in both IgAN patients (Graph 28 to Graph 31). These tendencies may only be confirmed by experiments of a larger number of patients.

Ideally, it had been useful to have data from the BD TruCount™ tubes. In that way, it would have been possible to obtain data for the absolute concentration of the subpopulations of dendritic cells and monocytes directly from the flow cytometric data. Information on blood leucocyte concentrations, including monocyte and lymphocyte concentrations, was of interest, as the percent wise distribution within parent the population (e.g. percentage of classical monocytes within the monocyte gate), could not itself reveal information on the level of blood concentrations. It is of interest to know, whether or not e.g. an increase in a monocyte subpopulation percentage was to be seen in the total blood concentration of monocytes and leucocytes in general. Given that no such data was obtained, data from the absolute leucocyte differential count was used in the calculations.

Since our attempt to determine absolute counts by the TruCount™ bead method failed, we unfortunately cannot provide absolute counts for the subpopulations of dendritic cells and monocytes from the control subjects. This is due to the fact that an absolute differential count was not performed on blood from the control subjects, only on blood from patients. However, in the literature, reference values for these

subpopulations can be found. The blood of healthy human adults contains approximately 0.45 $x10^9$ monocytes per litre (38). According to Graph 3, the blood monocyte concentration of the two patients differed in that patient 2 showed a lower blood monocyte concentration in comparison with patient 1. Patient 2 showed a concentration ranging closely to the reference value of 0.45 $x10^9$ monocytes/L at the first three measurements. Only the last measurement was elevated with reference to normal monocyte concentration. The same peak in blood concentration was seen for the non-classical and for the classical monocytes in Graph 4 and Graph 6. This indicated that the overall increase in monocyte blood concentration of patient 1 was the result from an increase in the number of non-classical monocytes and classical monocytes. The highest peak of monocyte blood concentration for patient 2 was seen at the first day of measurement, see Graph 3. When looking at Graph 4 to Graph 6, classical and intermediate monocytes seemed to be the contributing cell types for this overall blood monocyte concentration. It is noteworthy, that the peaks in blood monocyte concentrations of the two patients were, in part, due to an increase in classical monocytes.

The blood monocyte concentration of patient 2 seemed low at each measurement in comparison with the reference value (Graph 3). Likewise, lymphocyte concentration was lower in patient 2 than in patient 1 (Graph 2). Despite these values of concentration, total leucocyte blood concentration of patient 1 was similar to that of patient 2 (Graph 1). This indicated that granulocytes of the total leucocyte population were present in a higher amount in patient 2 compared to patient 1. Both patients had total leucocyte concentrations around the reference value of 6.19 $x10^9$ cells/L (39). When evaluating the monocyte and dendritic cell subpopulations and blood concentrations found in this experiment, it should be considered that the number of patients and control subjects was rather low. Clearly, more patients and control subjects and more measurements over a longer period of time would be preferred, as this would probably provide greater insight into the development over time and differences between subjects. It would have been interesting to see concentrations of the dendritic cell subpopulations in healthy individuals, since this is a necessity for evaluation of differences in IgAN patients and in control subjects.

Clear tendencies were observed in all subjects regarding the expression of HLA-DR on the different dendritic cell subpopulations (Graph 24 to Graph 27). $CD1c^+$ dendritic cells clearly had the highest expression of HLA-DR. $CD303^+$ cells showed the second level of HLA-DR expression, and the $CD141^+$ dendritic cells expressed least of the marker compared with the other subpopulations. Interestingly, peak levels of HLA-DR on $CD1c^+$ dendritic cells were higher for the control subjects than for the patients. Amongst the monocytes, HLA-DR expression was not as clearly defined between subpopulations as with dendritic cell suppopulations. In general, the intermediate monocytes had high expression of HLA-DR. Peak levels of HLA-DR expression on intermediate monocytes were slightly higher for control subjects than for the two patients. These results of HLA-DR expression indicate the possibility, that HLA-DR expression may be associated with IgAN. This result is in line with the findings of others that have demonstrated a genetic association with HLA and IgAN (40).

TLR4 expression of dendritic cells and monocytes did not reveal any clear difference between and within subjects. In several instances the TLR4 expression was found to be negative, both regarding monocyte and dendritic cell expression, see Graph 20 to Graph 23, and Graph 38 to Graph 41, respectively. Monocyte expression of TLR4 revealed increased values of intermediate and non-classical monocytes of patient 1, day

1, (see Graph 38) in comparison with the rest of the measurements of patient 1. In patient 2 and control subject 1intermediate monocytes also showed the greatest TLR4 expression between subpopulations.

The negative values of TLR4 expression indicated, that non-specific binding of the isotype control antibody was higher than the binding of the anti-TLR4 antibody. It was also clear that the PE-Cy7 isotype control used with the PE-Cy7 conjugated anti-TLR antibody exhibited a stronger binding than did the other isotype controls. Indeed, binding of PE-Cy5 conjugates has been demonstrated in a study by van Vugt et al., 1996 (41). It appears that when using PE-Cy5 conjugated monoclonal antibodies there is an effective binding of the PE-Cy5 conjugate of the antibody to the human CD64 receptor. In this way there is a risk that the fluorescence from PE-Cy5-conjugated antibodies does not reflect binding specificity to antigens of interest, but rather the binding of PE-Cy5 fluorochrome to CD64 on cells (41). It could be suspected, that there was a difference in the degree of PE-Cy7-fluorochrome-conjugation between the anti-TLR4 antibody and the isotype control antibody in this study, and that this contributed to a higher extent of non-specific binding of the isotype control antibody. In a situation like that, samples of very low values of fluorescence intensity caused by low TLR4 expression would probably be highly influenced by non-specific binding of the isotype control antibody. Median fluorescence intensities of an isotype control antibody with a high level of non-specific binding may, when retracted from the median fluorescence intensity of cells with little TLR4 expression, result in negative values of fluorescence. Indeed, the binding of the anti-TLR4 antibody does seem to be low in those instances where the value becomes negative after subtraction of the isotype value when looking on the original data (data not shown).

The undesirable binding of tandem PE-Cy5 conjugates was by others shown to be mediated by the CD64 receptor. A study of van Vugt et al. demonstrated that this binding could be inhibited by the addition of an anti-CD64 antibody (41). Since the PE-Cy7 fluorochrome is also a tandem dye (42), we suspect that the two fluorochromes are chemically related and hence, expect that the binding of the PE-Cy7 conjugates is also mediated by CD64. We therefore investigated the effect of adding an unconjugated anti-CD64 antibody to the antibody panel. No major changes were seen on the median fluorescence intensity of the PE-Cy-7 conjugated isotype antibody when staining with the anti-CD64 antibody. A study by Jahrsdörfer et al. in 2005 demonstrated, that phosphorothyoate oligonucleotides effectively suppress nonspecific binding of Cy5 conjugates to monocytes, more effectively than do anti-CD64 antibodies and Fc receptor blocking reagents (43). It may be suspected, that the binding epitope targeted by the anti-CD64 antibody used in present study was different from that of the PE-Cy7 conjugate. This would explain why the CD64 receptor blocking did not have any effect on the non-specific binding of the PE-Cy7 conjugated isotype control antibody.

The compensation of the present study was based on the use of BD CompBeads^{TM}. The staining of these beads was partly based on monoclonal antibodies of the experimental setup, partly on monoclonal antibodies of different specificity and manufacturer than in those of the experiment. Ideally, only the specific antibodies of the experiment should be used, since lot. numbers of antibodies may have slightly different fluorescence spectra (27). This was not possible, however, since dendritic cell enumeration was based on a commercially available antibody cocktail from which each single antibody could not be isolated and used in the compensation. The manufacturer of the antibodies of the cocktail did not provide separately antibodies like those of the cocktail, and as a consequence, other antibodies had to be used in the compensation. A future compensation setup should be based on each of the antibodies of the

experiment, which may eliminate the option of using commercially available antibody cocktails, but in return allow optimal compensation of the spectral overlaps of fluorescence.

As previously described, in multicolor flow cytometry, the flourochrome emission spectrum of a single fluorochrome can be affected by fluorescence spectra of additional colors in the same sample, despite proper compensation (36). The all-minus-one method is therefore preferable when staining cells with multiple colors, as it is the case of present study. By this approach of defining a negative control, it is possible to take into account that emission spectra may change with the presence of several colors. However, non-specific binding of e.g. tandem conjugates to cells must still be evaluated. All-minus-one plus isotype control is a way of combining the two ways of defining a negative population. This method includes the isotype control antibody of the antibody that is left out of the all-minus-one sample, and may be the optimal way of defining negative populations in studies involving multicolor flow cytometry.

Several optimizations of the protocol for urine monocyte enumeration were made in the course of this study, and this was essential to be able to analyze the presence of cells urine. Limited information is to be found on analysis of cells in urine (44), and the results of this study regarding monocytes in urine of IgAN patients seems to be unique to our knowledge. In healthy individuals, kidney function would be expected to be normal and glomerular damage non-existing. In present study no populations of granulocytes, monocytes, and lymphocytes were seen in the urine of control subjects. However, in one of the IgAN patients, leucocytes including monocytes were clearly present and could be analysed by flow cytometry. When looking at the subpopulations of these monocytes, it was revealed that classical monocytes comprised the majority of the monocytes. This result suggests further investigation of urine monocytes over time and during different states of disease in IgAN.

Conclusive Remarks

By this study it has been confirmed, that multicolor flow cytometry offers the opportunity of analysis of intermediate, non-classical, and classical monocytes, as well as plasmacytoid $CD303^+$, myeloid $CD1c^+$, and myeloid $CD141^+$ dendritic cells in IgAN patients.

Multicolor flow cytometry provides the capability of detection of multiple colors. However, reflections should be made in order to obtain useful and high quality data. In this study, it has been clearly shown, that the choice of fluorochrome-conjugated antibodies of the experimental antibody panel should be considered carefully, particularly when using fluorochromes that may show a high degree of non-specific binding to cells. In this study it was emphasized, that there is a need for careful quality controls when using tandem-conjugated antibodies.

The number of patients and control subjects for this type of experiment should be increased in a future study, as this would provide better opportunities for evaluation of cellular events in IgAN and in health. By also implementing the various improvements of the technique suggested above, great opportunities would arise to achieve more information on the condition of the innate immune system in IgAN.

Bibliography

1. **McCance, Kathryn L. and Huether, Sue E.** *Pathophysiology - The Biologic Basis for Disease in Adults and Children.* 5th edition. Missuori : Elsevier Mosby, 2006. 0-323-03507-8.

2. **Boyd, Joanna K., et al., et al.** An update on the pathogenesis and treatment of IgA nephropathy. 2012.

3. **Ziegler-Heitbrock, Loems, et al., et al.** Nomenclature of monocytes and dendritic cells in blood. *Blood.* 116, 2010, 16.

4. **Moldoveanu, Z., et al., et al.** Patients with IgA nephropathy have increased serum galactose-deficient IgA1 levels. *Kidney International.* 2007, 71, pp. 1148-1154.

5. **Barratt, Jonathan and Feehally, John.** Primary IgA Nephropathy: New Insights Into Pathogenesis. *Seminars in Nephrology.* 2011, 4, pp. 349-360.

6. **Boyd, Joanna K., et al., et al.** An update on the pathogenesis and treatment of IgA nephropathy. *Kidney International.* 2011.

7. **Tarelli, Edward, et al., et al.** Human serum IgA1 is substituted with up to six O-glycans as shown by matrix assisted laser desorption ionisation time-of-flight mass spectrometry. *Carbohydrate Research .* 2004, 339, pp. 2329-2335.

8. **Suzuki, Hitoshi, et al., et al.** IgA1-secreeting cell lines from patients with IgA nephropathy produce aberrantly glycosylated IgA1. *The Journal of Clinical Investigation.* 2008, 2, pp. 629-639.

9. **Allen, Alice C., et al., et al.** Mesangial IgA1 in IgA nephropathy exhibits aberrant O-glycosylation: Observations in three patients. *Kidney International.* 2001, 60, pp. 969-973.

10. **Hastings, M. Colleen, et al., et al.** Galactose-Deficient IgA1 in African Americans with IgA Nephropathy: Serum Levels and Heritability. *Clinical journal of the American Society of Nephrology.* 2010, 5, pp. 2069-2074.

11. **Smith, Alice C., et al., et al.** O-Glycosylation of Serum IgD in IgA Nephropathy. *Journal of the American Society of Nephrology.* 2006, 17, pp. 1192-1199.

12. **Smith, Alice C., et al., et al.** O-Glycosylation of Serum IgA1 Antibodies against Mucosal and Systemic Antigens in IgA Nephropathy. *Journal of the American Society of Nephrology.* 2006, 17, pp. 3520-3528.

13. **Novak, Jan, et al., et al.** Aberrant Glycosylation of IgA1 and Anti-Glycan Antibodies in IgA Nephropathy: Role of Mucosal Immune System. *Advances in Oto-Rhino-Laryngology.* 2011, 72.

14. **Coppo, Rosanna, et al., et al.** Innate immunity and IgA nephropathy. *Journal of Nephrology.* 23, 2010, 6, pp. 626-632.

15. **Launay , Pierre, et al., et al.** Fc a Receptor (CD89) Mediates the Development of Immunoglobulin A (IgA) Nephropathy Berger's Disease): Evidence for Pathogenic Soluble Receptor-IgA Complexes in Patients and CD89 Transgenic Mice. *The Journal of Experimental Medicine.* 191, 2000, 11, pp. 1999-2009.

16. **Grossetête, Béatrice, et al., et al.** Down-regulation of Fcα receptors on blood cells of IgA nephropathy patients: Evidence for a negative regulatory role of serum IgA. *Kidney International.* 1998, 53, pp. 1321-1335.

17. **Narita, Ichiei and Gejyo, Fumitake.** Pathogenic significance of aberrant glycosylation of IgA1 in IgA nephropathy. *Clinical and Experimental Nephrology.* 2008, 12, pp. 332-338.

18. **Cattran, Daniel C., et al., et al.** The Oxford classification of IgA nephropathy: rationale, clinicopathological correlations, and classification. *Kidney International.* 2009, 76, pp. 534-545.

19. **Hara, Masanori, Yanagihara, Toshio and Kihara, Itaru.** Cumulative Excretion of Urinary Podocytes Reflects Disease Progression in IgA Nephropathy and Schönlein-Henoch Purpura Nephritis. *Clinical Journal of the American Society of Nephrology.* 2007, 2, pp. 231-238.

20. **Couser, William G.** Basic and Translational Consepts of Immune-Mediated Glomerular Diseases. *Journal of the American Society of Nephrology.* 2012, 23.

21. **Coppo, R., et al., et al.** Toll-like receptor 4 expression is increased in circulating mononuclear cells of patients with immunoglobulin A nephropathy. *Clinican and Experimental Immunology.* 2009, 159, pp. 73-81.

22. **Myrphy, Kenneth.** *Janeway's Immunobiology.* 8th edition. New York : Garland Science, Taylor & Francis Group, 2012. 978-0-8153-4243-4.

23. **Netea, Mihai G. and van der Meer, Jos W.M.** Immunodeficiency and Genetic Defects of Pattern-Recognition Receptors. *The New England Journal of Medicine.* 2011, 364, pp. 60-70.

24. **Park, Hae Jeong, et al., et al.** Association between toll-like receptor 10 (TLR10) gene polymorphisms and childhood IgA nephropathy. *European Journal of Pediatrics.* 2011, 170, pp. 503-509.

25. **Macey, Marion G.** Principles of Flow Cytometry. *Flow Cytometry: Principles and Applications.* Totowa, New Jersey : Humana Press, 2007, 978-1-59745-451-3.

26. **Barnett, David and Reilly, John T.** Quality Control in Flow Cytometry. [book auth.] Marion G. Macey. *Flow Cytometry: Principles and Applications.* Totowa, New Jersey : Humana Press, 2007, 978-1-59745-451-3.

27. **BD Biosciences.** An Introduction to Compensation for Multicolor Assays on Digital Flow Cytometers. *BDbiosciences.com.* [Online] 2009. http://www.bdbiosciences.com/eu/support/resources/flowcytometry/index.jsp#techspecs.

28. **Givan, Alice L.** Flow cytometry: An Introduction. [book auth.] Teresa S. Hawley and Robert G. Hawley. *Flow Cytometry Protocols - Methods in Molecular Biology.* 3rd edition. s.l. : SpringerLink, 2011, 978-1-61737-950-5.

29. **Invitrogen.** Introduction to Flow Cytometry. *Invitrogen.com.* [Online] [Cited: May 15, 2012.] http://probes.invitrogen.com/resources/education/tutorials/4Intro_Flow/player.html.

30. **Maecker, Holden and Trotter, Joe.** Selecting Reagents for Multicolor Flow Cytometry. *BDBiosciences.com.* [Online] 2012. http://www.bdbiosciences.com/eu/support/resources/flowcytometry/index.jsp.

31. **Ekong, Theresa, et al., et al.** Technical influences on immunophenotyping by flow cytometry - The effect of time and temperature of storage on the viability of lymphocyte subsets. *Journal of Immunological Methods.* 1993, 164, pp. 263-273.

32. **BDbiosciences.** Techniques for Immune Function Analysis - Application handbook. *BDBiosciences.com.* [Online] 2nd edition, 2009. http://www.bdbiosciences.com/ecat/documentSearch.do?key=Handbook&prodCount=0&charset=utf-8&MatchAllTerms=true.

33. **Gratama, Jan W. , et al., et al.** Analysis of Factors Contributing to the Formation of Mononuclear Cell Aggregates (''Escapees'') in Flow Cytometric Immunophenotyping. *Cytometry.* 1997, 29, pp. 250-260.

34. **Brando, Bruno, et al., et al.** The "Vanishing Counting Bead" Phenomenon: Effect on Absolute CD341 Cell Counting in Phosphate-Buffered Saline-Diluted Leukapheresis Samples. *Cytometry.* 2001, 43, pp. 154-160.

35. **O'Gorman, Maurice R.G. and Thomas, Joanne.** Isotype Controls - Time to Let Go? *Cytometry.* 1999, 38, pp. 78-80.

36. **Baumgarth, Nicole and Roederer, Mario.** A practical approach to multicolor flow cytometry for immunophenotyping. *Journal of Immunological Methods.* 2000, 243, pp. 77-97.

37. **Battiston, Kyle G., et al., et al.** Differences in protein binding and cytokine release from monocytes on commercially sourced tissue culture polystyrene. *Acta Biomaterialia.* 2012, 8, pp. 89-98.

38. **Robbins, Clinton S. and Swirski, Filip K.** The multiple roles of monocyte subsets in steady state and inflammation. *Cellular and Molecular Life Sciencens.* 2010, 67, pp. 2685-2693.

39. **Sennels, Henriette P., et al., et al.** Diurnal variation of hematology parameters in healthy young males: The Bispebjerg study of diurnal variations. *Scandinavian Journal of Clinical and Laboratory Investigation.* 2011, 71, pp. 532-541.

40. **Feehally, John, et al., et al.** HLA Has Strongest Association with IgA Nephropathy in Genome-Wide Analysis. *Journal of the American Society of Nephrology.* 2010, 21, pp. 1791-1797.

41. **van Vugt, M.J., van den Herik-Oudijk, I.E. and van de Winkle, J.G.** Binding of PE-CY5 conjugates to the human high-affinity receptor for igG (CD64). *Blood.* 1996, 88.

42. **Bishop, James E., et al., et al.** A Setup System for Compensation: BD CompBeads plus BD FACSDiva Software. *BDBiosciences.com.* [Online] http://www.bdbiosciences.com/ecat/documentSearch.do?key=A+Setup+System+for+Compensation%3A&prodCount=0&charset=utf-8&MatchAllTerms=true.

43. **Jahrsdörfer, Bernd, Blackwell, Sue E. and Weiner, George J.** Phosphorothyoate oligodeoxynucleotides block nonspecific binding of Cy5 conjugates to monocytes. *Journal of Immunological Methods.* 2005, 297, pp. 259-263.

44. **Beatty, John D., et al., et al.** Urine dendritic cells: a noninvasive probe for immune activity in bladder cancer? *British Journal of Urology International.* 2004, 94, pp. 1377-1383.

45. **BD Biosciences.** BD Fluorescence Spectrum Viewer - A Multicolor Tool. *BDBiosciences.com.* [Online] 2012. http://www.bdbiosciences.com/eu/research/multicolor/spectrum_viewer/index.jsp.

Appendix A - Ethical Approval

Appendix B - Approval by the Danish Data Protection Agency

Appendix C - Compensation Matrix

Appendix D - Compensation: Negative and Positive Populations